Chapter 4
Chiral Perturbation Theory

Brian C. Tiburzi

Abstract The era of high-precision lattice QCD has led to synergy between lattice computations and phenomenological input from chiral perturbation theory. We provide an introduction to chiral perturbation theory with a bent towards understanding properties of the nucleon and other low-lying baryons. Four main topics are the basis for this chapter. We begin with a discussion of broken symmetries and the procedure to construct the chiral Lagrangian. The second topic concerns specialized applications of chiral perturbation theory tailored to lattice QCD, such as partial quenching, lattice discretization, and finite-volume effects. We describe inclusion of the nucleon in chiral perturbation theory using a heavy-fermion Euclidean action. Issues of convergence are taken up as our final topic. We consider expansions in powers of the strange-quark mass, and the appearance of unphysical singularities in the heavy-particle formulation. Our aim is to guide lattice practitioners in understanding the predictions chiral perturbation theory makes for baryons, and show how the lattice will play a role in testing the rigor of the chiral expansion at physical values of the quark masses.

4.1 Introductory Remarks

Prior to lattice-QCD computations, chiral perturbation theory (χPT) was the only method for doing high-precision low-energy QCD phenomenology. One crowning achievement of χPT is a procedure for the determination of ratios of the light-quark masses. These ratios can be determined using the experimentally measured hadron spectrum with small effects, such as isospin breaking from both strong and electromagnetic sources, treated in a systematic fashion, see [173]. In essence, χPT provides the tool to study the light-quark mass dependence of low-energy QCD

B.C. Tiburzi (✉)
Department of Physics, The City College of New York, New York, NY 10031, USA

Graduate School and University Center, The City University of New York, New York, NY 10016, USA

RIKEN BNL Research Center, Brookhaven National Laboratory, Upton, NY 11973, USA
e-mail: btiburzi@ccny.cuny.edu

H.-W. Lin, H.B. Meyer (eds.), *Lattice QCD for Nuclear Physics*, Lecture Notes in Physics 889, DOI 10.1007/978-3-319-08022-2_4

observables. As such, it is a tool that furnishes considerable insight for lattice QCD computations. The success of this model-independent description of low-energy QCD is limited in practice by the size of the physical light-quark masses compared to strong interaction scales. Lattice QCD computations are confronting predictions made by χPT. For the strange quark, there has been considerable debate about the efficacy of the $SU(3)$ chiral expansion, even in the meson sector. The chiral dynamics of the nucleon has not been conclusively exposed from lattice QCD computations. As lattice collaborations worldwide attain light quark masses, the chiral dynamics of low-lying hadrons will be rigorously tested.

We undertake the task of making a user-friendly introduction to χPT aimed at lattice practitioners, with a particular focus on the nucleon. From the outset, we stress that this chapter is not meant to be a comprehensive review of the field. By contrast, our aim is to provide a pedagogical introduction that will arm the reader with the tools necessary to investigate further. We hope to familiarize readers with the predictions that χPT makes for hadrons, and to advertise the role lattice QCD will play in assessing the chiral expansion at physical values of the quark masses. It is useful for the reader to be accustomed to the concept of an effective field theory, the study of which is possible through a number of excellent references. We recommend the textbooks [174, 175], and the summer school lectures [176]. For the specific topics covered in this chapter, we will suggest a few references for further study rather than provide an exhaustive list of the possibilities. Various exercises are scattered throughout the presentation. Some are simple and meant only as reminders, whereas others require more thought.

Our presentation is organized around four central topics. The first topic in Sect. 4.2 is key to the entire chapter and concerns the construction of the chiral Lagrangian. We consider the symmetry-breaking pattern of QCD for two light quark flavors, discuss the emergent Nambu-Goldstone bosons, and expose their universal low-energy dynamics through the effective chiral Lagrangian. The second topic is taken up in Sect. 4.3, where applications geared toward lattice QCD are the focus. Beyond providing quark-mass extrapolation formulae, χPT has been extended in various ways that are relevant for lattice gauge theory simulations. In particular, we address extensions needed to account for the partially quenched approximation to QCD, and modifications necessary to describe the effects of finite volume, as well as the effects of lattice discretization. Chiral dynamics of the nucleon is pursued in Sect. 4.4. Using a heavy-fermion Euclidean action, we show how to include the nucleon in χPT. Particular attention is paid to the quark-mass dependence of the nucleon mass, and to the phenomenology of the pion-nucleon sigma term. The issue of convergence is taken up as our final topic in Sect. 4.5. We remind the reader about the nature of asymptotic expansions, and the challenges inherent to assessing the convergence of the chiral expansion using phenomenology and lattice data. With such concerns in mind, we extend χPT to include the strange quark. We investigate how the chiral expansion of certain hyperon properties can be reorganized into a better perturbative expansion by re-summing strange-quark mass contributions. Finally, we address the appearance of unphysical singularities in the heavy-nucleon formulation and the need for threshold re-summations.

4.2 The Chiral Lagrangian

The possibility of building a phenomenological theory of low-energy QCD exists because there are unusually light particles in the hadron spectrum. Pions are the lightest hadrons, and they are well separated in energy from any other states or resonances. There is an elegant explanation, moreover, for the lightness of pions due to spontaneous breakdown of chiral symmetry. The physics underlying this explanation is the Nambu-Goldstone mechanism [177, 178], and allows us to construct systematically a phenomenological theory of pions. Chiral symmetry breaking and the construction of the chiral Lagrangian are the topics of this section.

4.2.1 Symmetries and Symmetry Breaking

The spectrum and properties of low-energy QCD are indicative both of its symmetries, and of its symmetry breaking. We begin with the case of QCD with two massless quark flavors, which will be identified as the up and down quarks. The action density for QCD can be written as the sum of contributions from matter and radiation fields, $\mathcal{L}_{\rm QCD} = \mathcal{L}_\psi + \mathcal{L}_{\rm YM}$, where the latter is the Yang-Mills action, $\mathcal{L}_{\rm YM}$. Our concern lies with the matter part of the action, $\mathcal{L}_\psi$, which has the form

$$\mathcal{L}_\psi = \sum_{i=1}^{2} \overline{\psi}_i \not{D} \psi_i \,. \tag{4.1}$$

Written this way, the action obviously possesses a global $U(2)$ flavor symmetry, but there is a larger symmetry group. To expose the further symmetries of the action, we define chiral projection matrices, $\mathcal{P}_{L,R} = \frac{1}{2}(1 \mp \gamma_5)$, which have all the usual properties expected of projectors. Right- and left-handed quark fields are then defined using chiral projectors, $\psi_{L,R} = \mathcal{P}_{L,R}\psi$. Consequently, the matter part of the QCD action can be written as

$$\overline{\psi} \not{D} \psi = \overline{\psi}_L \not{D} \psi_L + \overline{\psi}_R \not{D} \psi_R, \tag{4.2}$$

for the flavor-doublet quark field. This simple decomposition seems to make a profound statement: the chirality of a massless quark cannot be changed by gluon interactions. This is not exactly the full story, as we shall shortly see.

On account of the handed decomposition of the quark fields in Eq. (4.2), the symmetry group of the massless QCD action is *chiral*, having the form $U(2)_L \otimes U(2)_R$. Specifically for matrices $(L, R) \in U(2)_L \otimes U(2)_R$, we have the transformations $\psi_L \to L\psi_L$ and independently $\psi_R \to R\psi_R$. This transformation appears quite complicated in terms of the original Dirac fermion, $\psi \to (L\mathcal{P}_L + R\mathcal{P}_R)\psi$, but is nonetheless a symmetry of Eq. (4.1). An important subgroup of the chiral symmetry group is the vector subgroup, $U(2)_V$, which is the naïve flavor symmetry of the massless action. For a transformation with $L = R \equiv V$, we have simply $\psi \to V\psi$.

Additional subgroups of the chiral symmetry group are important. Consider the trivial group decomposition, $U(2)_L \otimes U(2)_R = U(1)_L \otimes U(1)_R \otimes SU(2)_L \otimes SU(2)_R$, achieved by removing the overall phase from each $U(2)$ transformation. Under the $U(1)_L \otimes U(1)_R$ subgroup, we have the simple phase transformations $\psi_L \to e^{i\theta_L}\psi_L$, and $\psi_R \to e^{i\theta_R}\psi_R$. In terms of the Dirac fermion field, we see

$$\psi \to \left[\frac{1}{2}\left(e^{i\theta_R} + e^{i\theta_L}\right) + \frac{1}{2}\left(e^{i\theta_R} - e^{i\theta_L}\right)\gamma_5\right]\psi. \tag{4.3}$$

The vector subgroup $U(1)_V \subset U(1)_L \otimes U(1)_R$ is specified by all phase transformations under which the left- and right-handed fields are re-phased identically, $\theta_R = \theta_L \equiv \theta$, and consequently $\psi \to e^{i\theta}\psi$. This global symmetry leads to the conservation of quark number (or equivalently baryon number). The orthogonal choice of phases, namely $\theta_R = -\theta_L \equiv \theta_5$, leads to the axial transformation of the quark field, $\psi \to e^{i\theta_5\gamma_5}\psi$, and generates the $U(1)_A$ symmetry of the action.

1 Consider the non-singlet axial transformation of the quark field, specified by $\psi_i \to (e^{i\phi^a\tau^a\gamma_5})_{ij}\psi_j$, with τ^a as isospin matrices. Is there a corresponding symmetry group for the massless QCD action?

As already alluded to, global symmetries generate classically conserved currents. According to the discussion so far, there should be three non-singlet left-handed currents, $J^a_{\mu,L} = \overline{\psi}_L\tau^a\gamma_\mu\psi_L$, three non-singlet right-handed currents, $J^a_{\mu,R} = \overline{\psi}_R\tau^a\gamma_\mu\psi_R$, in addition to the singlet vector current, $J_\mu = \overline{\psi}\gamma_\mu\psi$, and singlet axial-vector current, $J_{\mu 5} = \overline{\psi}\gamma_\mu\gamma_5\psi$. The regulated theory, however, is not invariant under flavor-singlet axial transformations. This is referred to as the chiral anomaly; because, at the quantum level, the singlet axial current is not conserved:

$$\partial_\mu J_{\mu 5}(x) = \partial_\mu J_{\mu,L}(x) - \partial_\mu J_{\mu R}(x) = -\frac{\alpha_s}{8\pi}\epsilon_{\mu\nu\rho\sigma}F^A_{\mu\nu}F^A_{\rho\sigma}, \tag{4.4}$$

in four dimensions. Of course, this is a subject well-known to lattice QCD. The chiral anomaly presents an essential obstacle in devising chirally invariant lattice regularizations for fermions. We suggest that readers unfamiliar with these issues consult [50].

Due to the chiral *asymmetry* in Eq. (4.4), we shall merely dismiss $U(1)_A$ from our discussion of symmetries. The definition of a regulated theory of massless QCD has a $U(1)_V \otimes SU(2)_L \otimes SU(2)_R$ symmetry, but this is not the final story. Pairing of quark chiralities is preferred by the vacuum state of QCD. This state should be viewed as the ground state of the quantum field theory, and the ground state generally need not respect the symmetries of the underlying theory. While perturbative QCD dynamics does not distinguish between quark chiralities, nonperturbatively, the ground state actually does, through the formation of a nonzero

vacuum expectation value (vev) of the chiral condensate, $\langle\overline{\psi}\psi\rangle = \langle\overline{\psi}_L\psi_R\rangle + \langle\overline{\psi}_R\psi_L\rangle \neq 0$. Indeed, massless quarks can change their chirality by scattering off a vacuum condensate of quarks and antiquarks paired by handedness. In this case, we refer to the chiral symmetry as being spontaneously broken by the vacuum. The formation of the condensate completely breaks the chiral symmetry of the theory, moreover, as the vev $\langle\overline{\psi}\psi\rangle$ is not invariant under any chiral subgroup of $SU(2)_L \otimes SU(2)_R$. The condensate is invariant under the vector subgroup, and thus, we have the symmetry breaking pattern $U(1)_V \otimes SU(2)_L \otimes SU(2)_R \longrightarrow U(1)_V \otimes SU(2)_V$.

At this point, we do not dismiss the non-singlet chiral symmetries as we did with the axial symmetry. It turns out that the case of spontaneously broken symmetries is considerably rich in physics. In fact, spontaneously broken global symmetries lead to massless excitations of the vacuum. This is the Nambu-Goldstone mechanism. In Fig. 4.1, we use a cartoon to elucidate the Nambu-Goldstone mechanism. The cartoon depicts the potential energy of a theory on a group manifold. The lowest-energy states are degenerate and form a circularly symmetric valley that reflects the rotational invariance of this theory; however, the physical vacuum of the theory is located at a particular angle. In this case, the rotational symmetry is spontaneously broken. When quantized, fluctuations about the vacuum state will correspond to particles. There are two distinct types: fluctuations up the hill are energetically costly and will correspond to massive excitations of the theory; on the other hand, fluctuations along the circular valley are energetically free and will correspond to massless excitations. For each of the broken generators, there is a flat direction in the vacuum manifold, and hence a massless particle. In QCD with two massless quarks, there should thus be three Nambu-Goldstone bosons.

Fig. 4.1 Cartoon depicting a spontaneously broken global symmetry. The global symmetry corresponds to rotations in the plane, for which the vacuum manifold exhibits a circular valley of energetically equivalent states. The physical vacuum sits in the valley at a particular angle

4.2.2 Chiral Dynamics

The dynamics governing Nambu-Goldstone modes is universal, depending only on the pattern of spontaneous symmetry breaking. To write down such a theory, we need to parameterize fluctuations associated with the broken generators. Mathematically we are parameterizing a coset of the group manifold. While our presentation is specific to the symmetry-breaking pattern of two-flavor QCD, we keep sufficient generality to allow extension to other cases of interest.

A nonzero value of the condensate specifies the location of the vacuum within the group manifold. Let us write the vev in the form

$$\langle \overline{\psi}_{jR} \psi_{iL} \rangle = -\lambda \delta_{ij}. \tag{4.5}$$

Under an $SU(2)_L \otimes SU(2)_R$ transformation, we see that the condensate is not invariant, $\langle \overline{\psi}_{jR} \psi_{iL} \rangle \to -\lambda (L R^\dagger)_{ij}$. However, the restriction of the condensate to the flavor identity, δ_{ij}, maintains invariance under the vector subgroup, $SU(2)_V$. The preservation of vector symmetries can be argued rigorously [179]. The value of the condensate λ is real, which implies that parity is not spontaneously broken. While we know experimentally that this is the case for QCD, the argument against spontaneous breaking of parity [180] does not have the status of a theorem because known loopholes exist. Nonetheless the form of the condensate in Eq. (4.5) dictates the pattern of spontaneous symmetry breaking.

To describe the Nambu-Goldstone modes, we treat the condensate as a locally valued field $\Sigma(x)$ that picks up a vev. The fluctuations about this value encode the Nambu-Goldstone bosons. Thus we promote

$$\delta_{ij} \longrightarrow \Sigma_{ij}(x) = \delta_{ij} + \cdots . \tag{4.6}$$

Because $\Sigma(x)$ describes the local fluctuations, we must have $\Sigma_{ij}(x) = [L(x) R^\dagger(x)]_{ij} = [e^{i\theta_L^a \tau^a} e^{-i\theta_R^b \tau^b}]_{ij}$ for the most general, local $SU(2)_L \otimes SU(2)_R$ fluctuation. Our concern, however, is not with all fluctuations, but with those corresponding to broken generators. As the vector subgroup remains intact, we seek to parameterize the coset $SU(2)_L \otimes SU(2)_R / SU(2)_V$. This can be achieved by simply restricting $\Sigma(x)$ not to lie in $SU(2)_V$. As such matrices are characterized by $\theta_L^a = \theta_R^a$, choosing the orthogonal combination $\theta_L^a = -\theta_R^a$ produces a parameterization of the coset. Writing $\theta_L^a \tau^a \equiv \phi / f$, we have the desired matrix

$$\Sigma = e^{2i\phi/f} = 1 + \frac{2i\phi}{f} + \cdots . \tag{4.7}$$

The Nambu-Goldstone modes appear in the coset field through ϕ, which is a traceless Hermitian 2×2 matrix, which we write in the form

$$\phi = \begin{pmatrix} \frac{1}{\sqrt{2}}\pi^0 & \pi^+ \\ \pi^- & -\frac{1}{\sqrt{2}}\pi^0 \end{pmatrix}. \tag{4.8}$$

From the transformation property of the coset under global chiral transformations, namely $\Sigma \to L\Sigma R^\dagger$, we can infer the transformation rule of the Nambu-Goldstone modes under the vector subgroup $SU(2)_V$. They transform as $\phi \to V\phi V^\dagger$, which establishes the isospin quantum numbers of ϕ; it contains an isotriplet of pions.

2 Deduce the discrete symmetry properties of the Nambu-Goldstone modes by analyzing the transformations of the coset field Σ.

In describing the vacuum fluctuations, we introduced a dimensionful parameter f. This parameter needs to be determined from experiment, and we will explain how at the end of this section. From a purely theoretical perspective, f controls whether fluctuations about the vacuum are Gaußian, hence, whether the Nambu-Goldstone modes are weakly interacting particles. To see this explicitly, we construct the action for the coset field. It is determined from all possible chirally invariant operators involving Σ, and derivatives of Σ. When the coset is expanded about its vev, the dynamics of massless pions should emerge. Using the transformation rule $\Sigma \to L\Sigma R^\dagger$, and realizing that $\Sigma^\dagger\Sigma = 1$, the chirally invariant combination involving the fewest number of derivatives is

$$\mathcal{L}_{\chi\text{PT}} = \frac{f^2}{8}\,\text{Tr}\left(\partial_\mu\Sigma^\dagger\partial_\mu\Sigma\right) = \frac{1}{2}\partial_\mu\pi^0\partial_\mu\pi^0 + \partial_\mu\pi^+\partial_\mu\pi^- + \mathcal{O}(1/f^2). \tag{4.9}$$

Expanding to quadratic order in the fields, we see that the numerical prefactor appended to the action ensures that the kinetic terms are canonically normalized, and indeed the theory describes three massless pions. This should come as no surprise; it is basically by design. Because the theory is nonlinear, however, expanding to a higher order produces multipion interactions. We will explain shortly how to treat these systematically.

So far our discussion has focused on QCD with two massless quarks, and there appear to be no such quarks found in nature. The up and down quarks have mass, however, their masses are considerably small compared to Λ_{QCD}. We can think about the discussion above as an approximation for the up and down quarks, and the natural question to ask becomes how to address the effect of nonvanishing quark masses. To answer this question, we return to the matter part of the QCD action, which has a mass term of the form

$$\Delta\mathcal{L}_\psi = m_q\overline{\psi}\psi = m_q\left(\overline{\psi}_R\psi_L + \overline{\psi}_L\psi_R\right), \tag{4.10}$$

for degenerate up and down quarks. This term breaks chiral symmetry in precisely the way the chiral condensate does, $SU(2)_L \otimes SU(2)_R \to SU(2)_V$. The theory of the Nambu-Goldstone modes should include terms which encode the explicit symmetry breaking introduced by the quark mass. The correct term to add to Eq. (4.9) is

$$\Delta\mathcal{L}_{\chi\text{PT}} = -m_q\lambda\,\text{Tr}\left(\Sigma^\dagger + \Sigma\right) = 4m_q\lambda\left[-1 + \frac{2}{f^2}\left(\frac{1}{2}\pi^0\pi^0 + \pi^+\pi^-\right)\right] + \cdots . \tag{4.11}$$

A few comments are in order. This term is not chirally invariant but maintains invariance under the vector subgroup, and thus shares precisely the same symmetries as the quark mass term in the QCD action. A new dimensionful parameter λ was introduced when writing down this term. It is not fixed by symmetries. We include here only a term at linear order in the quark mass. While there are terms proportional to m_q^2 which we will meet below, we are considering the perturbative expansion about the chiral limit, $m_q = 0$, and the linear-order term represents the leading contribution. From expanding out $\Delta\mathcal{L}_{\chi\text{PT}}$ to quadratic order in the fields, we see there is a contribution to the vacuum energy, and also a mass term for the pions, $m_\pi^2 = 8\lambda m_q/f^2$. Indeed, the pions are not exact Nambu-Goldstone bosons; the explicit breaking of chiral symmetry introduced by the quark mass term of the QCD action leads to a nonvanishing mass for the pions.

The vacuum energy must be due to the chiral condensate, the existence of which was an essential ingredient in our construction thus far. To expose this fact, we realize that the chiral condensate can be determined from the QCD partition function, $-\partial \log Z_{\text{QCD}}/\partial m_q = \langle\overline{\psi}\psi\rangle$. In order that the chiral Lagrangian be an effective theory for low-energy QCD, it must be that their partition functions match, $Z_{\chi\text{PT}} \simeq Z_{\text{QCD}}$. Of course this relation is not an equality, rather a statement about matching Green functions between the two theories (such foundational aspects to χPT are elucidated in [181]). As a result, we must have

$$\langle\overline{\psi}\psi\rangle = -\partial \log Z_{\chi\text{PT}}/\partial m_q. \tag{4.12}$$

On the left-hand side is the QCD vacuum expectation value, and on the right-hand side is the χPT expression evaluated in terms of the effective pion degrees of freedom. In order that the theories match in the chiral limit, we require $\langle\overline{\psi}\psi\rangle = -2N_f\lambda$. Because of parity and flavor invariance, this condition is simply $\langle\overline{\psi}_{jR}\psi_{iL}\rangle = -\lambda\delta_{ij}$; hence λ is exactly the same parameter introduced in Eq. (4.5) for the chiral condensate. Combining this identification with the expression for the pion mass, we have the Gell-Mann–Oakes–Renner relation, $f^2m_\pi^2 = 2m_q|\langle\overline{\psi}\psi\rangle|$.

4.2.3 Leading Order and Beyond

Let us summarize our findings so far. The dynamics of the approximate Nambu-Goldstone bosons of chiral symmetry breaking is described by the chiral Lagrangian, which has the form

$$\mathcal{L}_{\chi\text{PT}} = \frac{f^2}{8}\,\text{Tr}\left(\partial_\mu \Sigma^\dagger \partial_\mu \Sigma\right) - \lambda m_q\,\text{Tr}\left(\Sigma^\dagger + \Sigma\right) \tag{4.13}$$

and includes the leading terms involving the lowest number of derivatives and a single insertion of the quark mass. Up to quadratic order, we find the vacuum energy due to the chiral condensate and a theory of pions whose masses squared are linear in the quark mass. Beyond quadratic order, there are interaction terms, such as the quartic terms $\sim \frac{m_q\lambda}{f^4}\phi^4$ and $\sim \frac{1}{f^2}(\phi\partial_\mu\phi)^2$. As always, these higher-order interactions renormalize lower-order terms. For example, the four-pion interaction terms lead to a renormalization of the pion mass, which is shown in Fig. 4.2. Using the pion propagator, we schematically evaluate the contribution to the pion self-energy from the four-pion vertex with quark mass insertion,

$$\Delta m_\pi^2 \sim \frac{m_q\lambda}{f^4}\int_k \frac{1}{k^2+m_\pi^2} \sim \frac{m_q\lambda}{f^4}\left[\Lambda^2 + \frac{m_q\lambda}{f^2}\left(\log\Lambda^2 + \text{finite}\right)\right], \tag{4.14}$$

where Λ is a dimensionful ultraviolet cutoff scale. This result features a power-law divergence, which can be absorbed into a definition of the renormalized parameter λ; and, if we use dimensional regularization, this contribution will automatically be subtracted. Additionally, there is a logarithmic divergence which cannot be absorbed into a renormalization of the parameters we have thus far written down. The reason is that the divergence is proportional to the second power of the quark mass. To work at one-loop order, we require additional counterterms than the leading-order chiral Lagrangian can supply.

The requirement of additional terms should not be surprising, since the chiral Lagrangian represents a nonrenormalizable theory. This is not a fundamental limitation, however, because we expect its validity only at low energies. In order to make the theory useful in practice, we desire a scheme for organizing the infinite

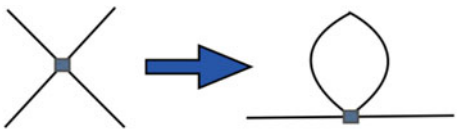

Fig. 4.2 Graphical depiction of the four-pion vertex. Forming a pion loop by contracting two of the external legs produces a divergent self-energy correction

number of local operators needed to renormalize the theory. Without such a power-counting scheme, the theory is of no practical use. In our exploration, we have been tacitly assuming a power counting. We have written down terms with the fewest number of derivatives, and the lowest number of quark mass insertions.

To make this formal, consider p to be a small momentum scale. A consistent loop expansion can be devised by counting the powers of derivatives and quark mass insertions as follows: derivatives count as one power, $\partial_\mu \sim p$, and quark masses count as two powers, $m_q \sim p^2$. The leading chiral Lagrangian written in Eq. (4.9) contains two terms both of order p^2. As a consequence, the pion propagator counts as order p^{-2}, and each of the four-pion interactions counts as order p^2. The remaining powers of momenta in a general Feynman diagram arise from loop integrals, which each contribute p^4 to the counting of powers of p. Now consider a Feynman diagram having L loops, I internal lines, and V vertices from the leading-order Lagrangian. The diagram must scale with the power $p^{4L-2I+2V}$. This power can be simplified using the Euler formula, $L = I - V + 1$, which gives the scaling p^{2L+2}. Thus, there is an ordered expansion in powers of p^2 if we consider the number of loops.

3 What happens to the power-counting argument in $d = 2$ and 6 dimensions? Do the results surprise you? Why is this question not asked about $d = 3$ or 5?

In considering part of the one-loop correction to the pion self-energy in Eq. (4.14), we found the result scales as $m_q^2 \sim p^4$, which is consistent with the general argument. At one-loop order, all contributions are of order p^4. To renormalize one-loop diagrams, we need higher-order local operators that also scale with four powers of p. These operators can only be formed from four derivatives, two derivatives and a quark mass insertion, or two quark mass insertions. At any order in the loop expansion, one requires only a finite number of higher-order counterterms to renormalize the theory. With this power counting, we can hence make sense of the nonrenormalizable theory.

To construct higher-order terms of the chiral Lagrangian with ease, the spurion trick proves useful. Let us first reconsider the leading-order effect of the quark mass in the chiral Lagrangian. The quark mass introduces explicit breaking of chiral symmetry and to include its effects, we wrote down a term which breaks the symmetry in precisely the same manner. Beyond leading-order, this task becomes rather difficult. Instead of this procedure, we promote the quark mass to a complex scalar field, denoted by s

$$\Delta\mathcal{L}_\psi = m_q \left(\overline{\psi}_R \psi_L + \overline{\psi}_L \psi_R\right) \longrightarrow \overline{\psi}_R s^\dagger \psi_L + \overline{\psi}_L s\, \psi_R, \tag{4.15}$$

and endow this field with a spurious transformation rule, $s \to LsR^\dagger$ which renders the quark mass term invariant. The procedure is then to construct all possible operators involving s that are invariant under chiral transformations. For example, with one insertion of s, the term $\mathrm{Tr}\left(\Sigma^\dagger s + s^\dagger \Sigma\right)$ is chirally invariant. At the end of the day, giving the scalar field a vev, $s = m_q + \cdots$, breaks chiral symmetry in precisely the way the quark mass does.

To construct the order p^4 chiral Lagrangian, we have the fields Σ and s, which have the transformations $\Sigma \to L\Sigma R^\dagger$, and $s \to LsR^\dagger$. Using these fields, we write down all possible p^4 terms that are chirally invariant. We also impose Euclidean invariance, and invariance under C, P and T transformations. Finally we replace the spurion field with its vev. The result is an effective Lagrangian encompassing the pattern of spontaneous and explicit symmetry breaking of QCD.

It is easy to construct invariant terms, for example $\left[\mathrm{Tr}\left(\Sigma^\dagger s - s^\dagger \Sigma\right)\right]^2$ is invariant under chiral transformations. When s picks up a vev, however, this term becomes $m_q^2\left[\mathrm{Tr}\left(\Sigma^\dagger - \Sigma\right)\right]^2$, which vanishes because Σ is an $SU(2)$ matrix. The difficult task becomes finding the minimal set of required terms. For two degenerate quarks, the corresponding fourth-order chiral Lagrangian can be written in the form

$$\begin{aligned}\mathcal{L}^{(4)}_{\chi\mathrm{PT}} = {} & L_1\left[\mathrm{Tr}\left(\partial_\mu \Sigma^\dagger \partial_\mu \Sigma\right)\right]^2 + L_2\,\mathrm{Tr}\left(\partial_\mu \Sigma^\dagger \partial_\nu \Sigma\right)\,\mathrm{Tr}\left(\partial_\nu \Sigma^\dagger \partial_\mu \Sigma\right) \\ & + L_3 \frac{m_q \lambda}{f^2}\,\mathrm{Tr}\left(\partial_\mu \Sigma^\dagger \partial_\mu \Sigma\right)\,\mathrm{Tr}\left(\Sigma^\dagger + \Sigma\right) + L_4 \frac{(m_q\lambda)^2}{f^4}\left[\mathrm{Tr}\left(\Sigma^\dagger + \Sigma\right)\right]^2 .\end{aligned} \tag{4.16}$$

The dimensionless coefficients of the operators, $\{L_i\}$, are free parameters referred to as low-energy constants. Often they are also called Gasser-Leutwyler coefficients, because the systematic investigation of chiral perturbation theory to one-loop order was carried out by them, see [182]. It is important to note that our Gasser-Leutwyler coefficients are not Gasser and Leutwyler's coefficients because of our differing parameterization of the coset manifold. The four low-energy constants provide the counterterms necessary to renormalize all one-loop graphs in χPT. When one considers external currents, additional terms become necessary.

4 Determine the effects of strong isospin breaking, $m_d \neq m_u$, on the chiral Lagrangian. At what order does the pion isospin multiplet split?

To illustrate the features of a one-loop computation in χPT, we perform the simplest possible one. This calculation is the chiral correction to the condensate. Beyond leading order, we have the operator expression

$$\langle \overline{\psi}\psi \rangle = -\frac{\partial Z_{\chi\mathrm{PT}}}{\partial m_q} = -4\lambda\left[1 - \frac{1}{f^2}\,\mathrm{Tr}\left(\phi^2\right)\right] + \text{c.t.}, \tag{4.17}$$

where c.t. denotes contributions from counterterms. Contracting the pions to form the bubble diagram yields a correction to the condensate

$$\Delta\langle\overline{\psi}\psi\rangle = \frac{12\lambda}{f^2}\int_k \frac{1}{k^2+m_\pi^2} = -\frac{12\lambda m_\pi^2}{(4\pi f)^2}\left[\frac{1}{\varepsilon} - \gamma_E + \log 4\pi + \log\frac{\mu^2}{m_\pi^2} + 1\right], \tag{4.18}$$

where we have computed the integral in $d = 4 - 2\varepsilon$ dimensions with $\varepsilon \ll 1$. The contribution from the counterterm can be determined using the fourth-order Lagrangian at tree level. Only the L_3 and L_4 terms survive differentiation with respect to the quark mass; furthermore, only the L_4 term contributes to the vacuum energy without requiring pion loops. Assembling the loop and local contributions after $\overline{\text{MS}}$, we arrive at the final result

$$\langle\overline{\psi}\psi\rangle = \langle\overline{\psi}\psi\rangle_{m_q=0}\left[1 + \frac{3m_\pi^2}{(4\pi f)^2}\left(\log\frac{\mu^2}{m_\pi^2} + 1\right) - \frac{m_\pi^2}{f^2}L_4(\mu)\right]. \tag{4.19}$$

Long-range corrections to the chiral-limit value of the condensate come with a chiral logarithm. The renormalization-scale dependence introduced by the logarithm is exactly compensated by the running of the Gasser-Leutwyler coefficient, $L_4(\mu)$; specifically, it must satisfy the renormalization group equation, $\mu^2\frac{d}{d\mu^2}L_4 = \frac{3}{16\pi^2}$.

Generally, χPT can be used to compute the quark-mass corrections to various low-energy observables. Expressions for these observables will involve their chiral-limit values plus chiral logarithms that are calculable from the one-loop (and higher) diagrams. Additionally, there are local contributions from higher-dimensional operators that are required to renormalize the theory. The low-energy constants introduced require experimental data or lattice calculations to determine. Beyond the chiral condensate, which we found has a chiral expansion of the form $\langle\overline{\psi}\psi\rangle = A\left[1 + B\,m_q\left(\log m_q + C\right)\right]$, a few examples are the pion mass, which has a chiral expansion of the form $m_\pi^2 = A\,m_q\left[1 + B\,m_q\left(\log m_q + C\right)\right]$, and the scattering length for $I = 2$ pion scattering, which has a chiral expansion of the form $a_{\pi\pi}^{I=2} = A\sqrt{m_q}\left[1 + B\,m_q\left(\log m_q + C\right)\right]$.

4.2.4 External Fields

The determination of further quantities, such as electroweak observables, requires the inclusion of external fields. To accomplish this, we return to the QCD action and use the gauge principle to include external left- and right-handed fields

$$\mathcal{L}_\psi = \overline{\psi}_L \not{D}_L \psi_L + \overline{\psi}_R \not{D}_R \psi_R, \tag{4.20}$$

with the handed gauge-covariant derivatives specified by $(D_\mu)_L = \partial_\mu + igA_\mu + iL_\mu$, and $(D_\mu)_R = \partial_\mu + igA_\mu + iR_\mu$. For example, an external electromagnetic field is

included by choosing the left- and right-handed gauge fields as $L_\mu = R_\mu = QeA_\mu^{\rm em}$, with $A_\mu^{\rm em}$ the photon field, Q the electric-charge matrix, and e the unit of electric charge. The gauged theory has a local chiral invariance under which the quark fields transform as $\psi_L \to L(x)\psi_L$, and $\psi_R \to R(x)\psi_R$. The external fields must correspondingly transform according to the rules: $L_\mu \to L(x)L_\mu L^\dagger(x) + i[\partial_\mu L(x)]L^\dagger(x)$ for the left-handed gauge field, and $R_\mu \to R(x)R_\mu R^\dagger(x) + i[\partial_\mu R(x)]R^\dagger(x)$ for the right-handed gauge field.

To include external fields in χPT, we promote the global chiral invariance to a local one. The coset field consequently has the transformation $\Sigma \to L(x)\Sigma R^\dagger(x)$, and it becomes efficacious to define a chirally covariant derivative that satisfies the transformation rule $D_\mu\Sigma \to L(x)[D_\mu\Sigma]R^\dagger(x)$. Using the transformations of the external gauge fields, the chirally covariant derivative must have the form

$$D_\mu\Sigma = \partial_\mu\Sigma + iL_\mu\Sigma - i\Sigma R_\mu^\dagger. \tag{4.21}$$

If we count the external gauge fields as order p in the power counting, then $D_\mu \sim p$, and the leading-order chiral Lagrangian has exactly the same form as in Eq. (4.9), with the replacement $\partial_\mu \to D_\mu$. At higher orders, one carries out this replacement to ensure gauge invariance; however, there are additional operators that are required too.

As an application of including external fields in χPT, we shall consider the weak decay of the pion. The charged pion decay process, $\pi \to \mu + \nu_\mu$, arises from the W-boson of the weak interaction, as shown in Fig. 4.3. The left-handed quark current that couples to the weak boson is contained in the interaction Lagrangian

$$\Delta\mathcal{L}_W = W_\mu^- J_{\mu,L}^+, \quad \text{with} \quad J_{\mu,L}^+ = \overline{\psi}_L \tau^+ \gamma_\mu \psi_L. \tag{4.22}$$

The strong interaction part of the decay factorizes into a matrix element between the left-handed current and the pion,

$$\langle 0|J_{\mu,L}^+|\pi(\boldsymbol{p})\rangle = ip_\mu f_\pi, \tag{4.23}$$

where we have parameterized the matrix element based on Euclidean invariance and discrete symmetries. As a result, the parameter f_π, known as the pion decay constant, is a real-valued parameter. While the weak interaction occurs at the scale $\mu \sim M_W$, the nonperturbative QCD matrix element should be evaluated at a scale $\mu \sim \Lambda_{\rm QCD}$. In quark-mass–independent renormalization schemes, however, the non-singlet left-handed current is conserved and, therefore, has vanishing anomalous dimension. Consequently, the pion decay constant is independent of scale.

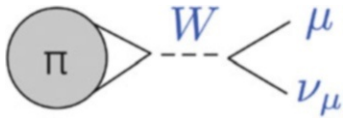

Fig. 4.3 Weak decay of the charged pion through the W-boson and its subsequent decay

With the nonperturbative physics parameterized, evaluating the decay process is a standard quantum field theory exercise, which gives the decay width

$$\Gamma_{\pi\to\mu+\nu_\mu} = \frac{G_F^2}{8\pi} f_\pi^2 \, m_\mu^2 m_\pi |V_{ud}|^2 \left(1 - \frac{m_\mu^2}{m_\pi^2}\right)^2 , \tag{4.24}$$

from which we infer the value $f_\pi = 132\,\text{MeV}$. We can use this value to fix one of the low-energy constants of χPT. The left-handed quark current matches onto operators in the effective theory. Using the order-p^2 chiral Lagrangian, we have

$$J^a_{\mu,L} = \frac{\partial \mathcal{L}_{\chi\text{PT}}}{\partial L^a_\mu}\Big|_{L_\mu = R_\mu = 0} = \frac{f^2}{4} \operatorname{Tr}\left(i\tau^a \Sigma \partial_\mu \Sigma^\dagger\right) = \frac{f}{2} \operatorname{Tr}\left(\tau^a \partial_\mu \phi\right) + \cdots \tag{4.25}$$

Computing the pion decay constant in the effective theory at tree level gives us the matching condition, $f_\pi = f$. A one-loop computation will produce chiral corrections to the matching of the form $f_\pi = f\left[1 + Bm_q\left(\log m_q + C\right)\right]$, whereby we see f is the chiral-limit value of the pion decay constant.

While f happens to show up in the weak decay of the charged pion, this parameter plays an important role in strong-interaction physics. The size of f controls the efficacy of the chiral expansion, because it governs the size of non-Gaußian fluctuations about the vacuum. Let us define the chiral symmetry breaking scale $\Lambda_\chi = 2\sqrt{2}\pi f \approx 1.2\,\text{GeV}$. Because our power-counting scheme gives us an expansion in the number of loops, we see each loop in four dimensions will be accompanied by a factor of $1/\Lambda_\chi^2$. Thus dimensionless parameters governing the size of chiral corrections are m_π^2/Λ_χ^2, and p^2/Λ_χ^2, where p is the momentum involved in a typical process.

5 The masses of hadrons are affected by electromagnetism (Fig. 4.4). Construct all leading-order electromagnetic mass operators by promoting the electric charge matrix to fields transforming under the chiral group. (Notice that no photon fields will appear in the electromagnetic mass operators, because there are no *external* photon lines.) Which pion masses are affected by the leading-order operators? Finally, give an example of a next-to-leading-order operator, or find them all.

Fig. 4.4 Feynman diagrams depicting long-range QED corrections to the pion mass

4.3 Applications Tailored to Lattice QCD

Above, we have detailed the construction of the chiral Lagrangian, and investigated the computation of low-energy QCD observables using this effective theory. The results of such computations are parametrizations of the quark-mass dependence of low-energy observables, with coefficients that must ultimately be determined from phenomenology or lattice QCD computations. The parameterizations, moreover, can be used for the extrapolation of lattice-QCD data at unphysical light-quark masses to their physical values. There are additional applications of chiral perturbation theory tailored to lattice QCD. In this section, we consider the partially quenched approximation to QCD, effects of finite lattice volumes, and effects of finite lattice spacings.

4.3.1 Partially Quenched QCD

Treating the valence and sea quarks in QCD differently is unphysical; however, it can be quite natural from a practical, numerical point of view. Consider the evaluation of the matrix element of an operator $\mathcal{O}$ between hadron states H and H'. On the lattice, one computes Wick contractions between source and sink, which schematically have the form

$$\langle H'|\mathcal{O}|H\rangle_{\mathrm{QCD}} = \int \mathcal{D}A_\mu \ \mathrm{Det}\left(\not{D} + m_q\right) e^{-S[A_\mu]} \frac{1}{\not{D} + m_q} \cdots \frac{1}{\not{D} + m_q}. \tag{4.26}$$

In the early days of lattice QCD, one encountered the quenched approximation, in which the above matrix element is calculated without the quark determinant,

$$\langle H'|\mathcal{O}|H\rangle_{\mathrm{QQCD}} = \int \mathcal{D}A_\mu \ e^{-S[A_\mu]} \frac{1}{\not{D} + m_q} \cdots \frac{1}{\not{D} + m_q}. \tag{4.27}$$

This approximation has various theoretical complications; however, a number of physical observables are insensitive to effects of the QCD vacuum polarization. One way to view the quenched approximation to QCD is a version of QCD with valence and sea quarks, where the latter have masses that are above the ultraviolet cutoff scale. This view suggests another approximation to QCD, the partially quenched approximation, in which the hadronic matrix element of $\mathcal{O}$ is calculated as

$$\langle H'|\mathcal{O}|H\rangle_{\mathrm{PQQCD}} = \int \mathcal{D}A_\mu \ \mathrm{Det}\left(\not{D} + m_{\mathrm{sea}}\right) e^{-S[A_\mu]} \cdot \frac{1}{\not{D} + m_{\mathrm{val}}} \cdots \frac{1}{\not{D} + m_{\mathrm{val}}}. \tag{4.28}$$

Matrix elements calculated in this approximation reduce to QCD matrix elements by choosing the valence and sea quark masses to be degenerate, $m_{\text{val}} = m_{\text{sea}}$. The partially quenched paradigm is useful to have in mind when considering mixed-action simulations, where in essence one replaces $\text{Det}\left(\not{D} + m_q\right) \to \text{Det}\left(\not{D}_{\text{sea}} + m_q\right)$, and when considering the effects of neglecting quark-disconnected diagrams.

For PQQCD computations, the natural questions are whether the quark-mass dependence can be addressed in a model-independent fashion, and whether artifacts of the approximation can be removed in order to connect with QCD physics. The theoretical technique to address such questions was first suggested for QQCD in [183]. The basic idea is as follows. A theory that reproduces the matrix element in Eq. (4.28) contains bosonic quarks, $\tilde{\psi} = \begin{pmatrix} \tilde{u} \\ \tilde{d} \end{pmatrix}$, in addition to fermionic quarks, the valence quarks $\psi = \begin{pmatrix} u \\ d \end{pmatrix}$, and the sea quarks $\psi' = \begin{pmatrix} u' \\ d' \end{pmatrix}$, namely

$$\begin{aligned} \mathcal{L}_{\text{PQQCD}} &= \overline{\psi}\left(\not{D} + m_{\text{val}}\right)\psi + \overline{\psi}'\left(\not{D} + m_{\text{sea}}\right)\psi' + \overline{\tilde{\psi}}\left(\not{D} + m_{\text{val}}\right)\tilde{\psi} \\ &\equiv \overline{\Psi}\left(\not{D} + m_{\text{PQ}}\right)\Psi, \end{aligned} \tag{4.29}$$

where Ψ is the graded vector, $\Psi = \begin{pmatrix} \psi \\ \psi' \\ \tilde{\psi} \end{pmatrix}$, whose upper components ψ and ψ' are Grassmann fields, and lower components $\tilde{\psi}$ are bosonic fields. The bosonic functional integration produces a factor of $\text{Det}\left(\not{D} + m_{\text{val}}\right)^{-1}$ which cancels the determinant produced from the fermionic valence quark functional integration. As a result, a net determinant factor is produced only from the sea quarks. In computing operator matrix elements, the external sources are built from valence quarks, and their contribution to the vacuum polarization is exactly canceled by the degenerate bosonic quarks. The vacuum polarization arises solely from sea quarks, see Fig. 4.5.

These observations were employed to construct PQχPT [184–186]. The relation of parameters in the partially quenched chiral Lagrangian to those in χPT was rigorously established in [187, 188], where further technical details can be found. As a caveat, we will summarize the approach with less rigor, and the careful reader will want to review the technical details in order to confidently utilize the results.

Fig. 4.5 Partially quenched QCD vacuum polarization at one loop. *Thin lines* depict valence quarks ψ, *dashed lines* depict bosonic quarks $\tilde{\psi}$, and *thick lines* depict sea quarks ψ'. Due to mass degeneracy between valence and bosonic quarks, the net contribution arises solely from the sea

In the massless limit, the partially quenched Lagrangian exhibits graded symmetries. These are symmetries under which bosonic and fermionic fields transform into one another. We write the partially quenched quarks as $\Psi_A = \begin{pmatrix} \psi_a \\ \phi_\alpha \end{pmatrix}$, with all fermionic quarks packaged in ψ_a, and bosonic quarks in ϕ_α. Under a graded unitary transformation, $\mathcal{U} \in U(4|2)_V$, we have the quark transformation $\Psi_A \to \mathcal{U}_{AB}\Psi_B$. Written in blocks, $\mathcal{U}$ must have the form

$$\mathcal{U}_{AB} = \begin{pmatrix} \mathcal{A}_{4\times4} & \mathcal{B}_{4\times2} \\ \mathcal{C}_{2\times4} & \mathcal{D}_{2\times2} \end{pmatrix}_{AB}, \tag{4.30}$$

where $\mathcal{A}$ and $\mathcal{D}$ are ordinary matrices, while $\mathcal{B}$ and $\mathcal{C}$ are matrices with Grassmann entries. This grading ensures that the transformed fermionic fields, for example, remain fermionic. Suppose $\mathcal{M}_{AB}$ is a supermatrix transforming under the adjoint, $\mathcal{M}_{AB} \to [\mathcal{U}\mathcal{M}\mathcal{U}^\dagger]_{AB}$, then the invariant graded trace (supertrace) is given by

$$\mathrm{Str}\,(\mathcal{M}) \equiv \sum_A (-)^{g(A)}\mathcal{M}_{AA} = \sum_a \mathcal{M}_{aa} - \sum_\alpha \mathcal{M}_{\alpha\alpha}, \tag{4.31}$$

where the grading factors are defined by $g(a) = 0$ and $g(\alpha) = 1$.

6 Show that the graded trace is invariant under graded unitary transformations.

The partially quenched χPT Lagrangian is constructed by taking into account the pattern of spontaneous and explicit breaking of chiral symmetry in PQQCD. Schematically the massless PQQCD Lagrangian possesses a graded chiral symmetry of the form $SU(4|2)_L \otimes SU(4|2)_R$ that we assume is spontaneously broken down to the vector subgroup, $SU(4|2)_V$. The emerging Nambu-Goldstone bosons live in the coset, $\Sigma = e^{2i\Phi/f}$, where we take Φ to be a $U(4|2)$ matrix

$$\Phi = \begin{pmatrix} \phi_{\bar{\psi}\psi} & \phi_{\bar{\psi}\psi'} & \phi_{\bar{\psi}\tilde{\psi}} \\ \phi_{\bar{\psi}'\psi} & \phi_{\bar{\psi}'\psi'} & \phi_{\bar{\psi}'\tilde{\psi}} \\ \phi_{\tilde{\bar{\psi}}\psi} & \phi_{\tilde{\bar{\psi}}\psi'} & \phi_{\tilde{\bar{\psi}}\tilde{\psi}} \end{pmatrix}, \tag{4.32}$$

which contains both bosonic and fermionic mesons. Taking into account the explicit chiral symmetry breaking due to the PQQCD mass matrix m_{PQ}, we arrive at the chiral Lagrangian

$$\mathcal{L}_{\mathrm{PQ}\chi\mathrm{PT}} = \frac{f^2}{8}\,\mathrm{Str}\left(D_\mu\Sigma^\dagger D_\mu\Sigma\right) - \lambda\,\mathrm{Str}\left(m_{\mathrm{PQ}}\Sigma^\dagger + \Sigma m_{\mathrm{PQ}}\right) + \frac{1}{2}\mu_0^2\left[\mathrm{Str}\,(\Phi)\right]^2. \tag{4.33}$$

Notice we retain the singlet meson in the theory, $\Phi_0 = \mathrm{Str}\,(\Phi) = \eta'_{\mathrm{val}} + \eta'_{\mathrm{sea}} - \tilde{\eta}'$. This is only a convenient device. In PQQCD, the $U(1)_A$ symmetry is anomalous just as in QCD, and the flavor-singlet meson needs to be integrated out of the low-energy theory. Computation of the flavor-neutral meson two-point functions can be carried out easily with the mass term, μ_0^2, treated as an interaction and summed to all orders. The limit $\mu_0 \to \infty$ produces the correct theory corresponding to $SU(4|2)_L \otimes SU(4|2)_R$. The resulting neutral-meson propagators have double poles, which indicate unitary violation in the partially quenched theory. Unitarity is never demanded of an effective theory, and the claim is that the peculiar lack of unitarity of PQQCD is captured at low energies by PQχPT.

After the singlet meson has been integrated out, one can establish that the parameters f and λ of the leading-order PQχPT Lagrangian are numerically identical to those in χPT. The proof utilizes a trick. One considers the computation of quantities involving mesons flavored only with sea quarks. In this sector of the theory, PQQCD Green functions are identical to QCD Green functions with $m_q = m_{\mathrm{sea}}$. As a result, the exact parameters of χPT must appear in PQχPT, although the latter also contains additional parameters. These further terms must be accounted for, and their effects removed to recover QCD physics from PQQCD. Additionally, the valence- and sea-quark mass dependence is described by PQχPT, and must be utilized to extrapolate lattice data to the unitary point, $m_{\mathrm{sea}} = m_{\mathrm{val}}$.

7 Find the tree-level masses of all charged mesons using partially quenched chiral perturbation theory.

4.3.2 Effects of Finite Volume

Lattice QCD computations by necessity utilize finite volumes. Because pions are the lightest hadrons, the long-range physics of low-energy QCD is modified predominantly due to pion effects. In considering finite-volume field theories, we must specify boundary conditions and choose them to be periodic for simplicity. Such boundary conditions lead to a number of salient features: the finite volume action is single valued on a hypertorus, consequently there are no surface terms; discrete translational symmetry is maintained, consequently periodic boundary conditions are not renormalized.

Let ϕ be a generic field satisfying $\phi(x + L) = \phi(x)$, where L is the length of each spacetime direction. The Fourier-mode expansion, $\phi(x) = \int_k e^{ikx}\phi_k$, coupled with periodicity leads to momentum quantization, $k = \frac{2\pi n}{L}$, where n is any integer. This simplicity is quite profound. All of the effects of finite volume follow from the quantization condition. As an example, consider Euclidean $SO(4)$ invariance.

On a finite periodic volume, this continuous invariance is reduced to a discrete permutation symmetry. The rest-frame matrix element measuring the electric charge of a particle, $\langle\phi(0)|J_\mu|\phi(0)\rangle = Q\delta_{\mu 4}$, does not lead to the usual current in a frame moving with velocity $\boldsymbol{v}$, so that $\langle\phi(v)|\boldsymbol{J}|\phi(v)\rangle \neq Q\boldsymbol{v}$, due to the lack of boost covariance. This may seem paradoxical, because gauge invariance, the Ward-Takahashi identity, and the Ward identity place constraints on the matrix elements of conserved currents. Ordinarily these three notions are used interchangeably; however, the Ward identity ceases to be valid. This finite-volume effect is exposed in [189]. Here, we explore finite-volume effects on pion dynamics in two distinct regimes.

4.3.2.1 Zero Pion Momentum

Strictly speaking, spontaneous symmetry breaking does not occur in finite volume. The reason is that spontaneous symmetry breaking is a classical phenomenon requiring infinitely many degrees of freedom. In quantum mechanics, a state prepared in one of a few degenerate ground states will acquire an admixture of the other states due to quantum tunneling. The dynamics of the theory governs tunneling, and over time the state will end up in a symmetric superposition of the degenerate ground states. In quantum field theory, the tunneling probability depends on the transition from two configurations on the group manifold, a and b. For uniform configurations, the tunneling probability, $\mathcal{P} \sim \exp\left(-V\int_a^b \mathcal{V}(\phi)d\phi\right)$, is exponentially suppressed by the infinite spacetime volume V. At finite volume, such tunneling occurs, and the vacuum state will tunnel symmetrically, thereby completely respecting the symmetric dynamics of the underlying action. In QCD, chiral symmetry can be restored at finite volume, and the effect can be deduced by carefully considering the effect of momentum quantization on pion dynamics.[1]

To expose the mechanism behind chiral symmetry restoration, we consider the computation of the chiral condensate in finite-volume χPT at one-loop order. To use χPT in a finite volume, the box size cannot be smaller than the chiral symmetry breaking scale, that is $L \gg \Lambda_\chi^{-1}$, otherwise there is no low-energy dynamics in the theory. Above, in Eq. (4.19), we calculated the infrared chiral logarithm, $\sim m_\pi^2 \log m_\pi^2$, which modifies the value of the chiral condensate away from the chiral limit. In finite volume, the one-loop diagram now requires a momentum mode sum rather than a momentum integral:

[1] Analogous to the situation at finite volume is the finite-temperature case, $\beta = 1/T < \infty$. The equilibrium quantum field theory has a path-integral representation in terms of the QCD action defined with a compact Euclidean time, $0 < x_4 < \beta$. Statistics demands periodic boundary conditions for bosons, and anti-periodic boundary conditions for fermions. In χPT, the restoration of chiral symmetry at finite temperature is linked with the Matsubara modes of the pions.

$$\frac{1}{f^2L^4}\sum_{n_\mu=-\infty}^{\infty}\frac{1}{\left(\frac{2\pi n_\mu}{L}\right)^2+m_\pi^2}=\frac{1}{(fL)^2}\left[\frac{1}{(m_\pi L)^2}+\sum_{n_\mu\neq 0}\frac{1}{4\pi^2 n_\mu^2+(m_\pi L)^2}\right]. \tag{4.34}$$

In the sum, we have separated out the contribution from the zero-momentum mode, $n_\mu = (0,0,0,0)$. The one-loop correction vanishes in infinite volume when $m_\pi = 0$, while in finite volume the zero mode leads to singular behavior in the infrared.

The longest-range piece of the pions, their zero-momentum mode, has become strongly coupled. The effect must be treated nonperturbatively and requires reformulating the power counting at finite volume [190]. Let ε denote a generically small quantity. We assign the counting of physical parameters as follows. The length L is considered large, and so $\frac{1}{L}$ counts as ε. The pion mass is chosen to count as $m_\pi \sim \varepsilon^2$. This creates a dichotomy in the leading-order Lagrangian: the derivative vertices count as $\partial_\mu\partial_\mu \sim \varepsilon^2$, unless they are zero modes, whereas the quark mass insertion is considered smaller, $m_q \sim m_\pi^2 \sim \varepsilon^4$. As a consequence, the pion propagator has two very distinct pieces. The propagation of zero modes counts as ε^{-4}, while nonzero modes count as ε^{-2}. The enhancement of zero modes over nonzero modes in the power counting encapsulates the chiral limit at finite volume.

To count powers of ε for a generic Feynman diagram, we further require the counting of loop factors. Each loop requires the mode summation $\frac{1}{L^4}\sum_{n_\mu}$ which counts as ε^4. For a diagram with I internal lines, V vertices from the leading-order Lagrangian, and L loops, we have now various scalings with ε possible depending on whether derivatives or quark mass insertions are at each vertex, and whether zero or nonzero modes are propagating. Diagrams having a quark-mass insertion at each vertex and only zero modes propagating count as $\varepsilon^{4L+4V-4I}$, which simplifies dramatically to ε^4 on account of the Euler identity. On the other hand, diagrams with only derivative vertices and nonzero modes propagating count as $\varepsilon^{4L+2V-2I} = \varepsilon^{2L+2}$. The nonzero momentum modes of the pion still obey a loop expansion. Diagrams with only zero modes, however, are all equally important.

8 Do the leading-order four-pion interactions allow mixing of zero and nonzero modes? Draw all one- and two-loop diagrams for the chiral condensate and count powers of ε.

The ε-regime power counting requires that the zero-momentum mode be treated nonperturbatively. Fortunately, the zero-momentum mode is the simplest mode, and can be separated out from the coset using the decomposition $\Sigma(x) = \Sigma_0 e^{2i\tilde{\phi}(x)/f}$, where Σ_0 is the zero mode, and the nonzero modes reside in $\tilde{\phi}(x)$. Taking into account only the zero mode, the partition function for χPT becomes a matrix model,

$$Z_{\chi\mathrm{PT}} = \int \mathcal{D}\Sigma_0 \, e^{\frac{1}{2}s\,\mathrm{Tr}\left(\Sigma_0^\dagger + \Sigma_0\right)}, \tag{4.35}$$

where the matrix integral represents averaging the direction of the chiral condensate over the coset manifold. The scaling variable s includes the spacetime volume V, and is defined by $s = 2m_q\lambda V = \frac{1}{4}(fL)^2(m_\pi L)^2$. In $SU(2)$, the matrix integral can be evaluated in terms of a modified Bessel function, $Z_{\chi\mathrm{PT}} = \frac{1}{s}I_1(2s)$. This result, in turn, can be used to find the behavior of the chiral condensate as a function of s in the ε-regime via Eq. (4.12). We plot this dependence in Fig. 4.6. If one takes the chiral limit at finite volume, chiral symmetry is restored. Chiral symmetry breaking can be achieved in a finite volume provided the pion Compton wavelength is small compared to the lattice size, $\frac{1}{m_\pi} \ll L$, for which s is large and the identity matrix becomes the preferred direction for the condensate to point.

4.3.2.2 Zero Pion Winding

To avoid finite-volume restoration of chiral symmetry, we require $m_\pi L \gg 1$ to ensure the zero-momentum modes of pions do not become strongly coupled. Provided this condition is met, finite-volume corrections should be perturbatively small, as pions only interact weakly with their periodic images. With small pion Compton wavelengths, we need to focus on corrections near zero pion winding number, rather than on zero pion momentum. This can be achieved systematically using p-regime power counting [191].

In the p-regime, we no longer distinguish between zero and nonzero momentum modes of pions. As a result, we count the pion mass and derivatives at the same order, $m_\pi \sim p$, and $\partial_\mu \sim \frac{1}{L} \sim p$. This is the same power counting as in infinite volume. The only exception is that the quantization condition restricts available momenta. Consequently, the pion propagator and leading-order vertices scale with the same power of p as in infinite volume. Each loop brings along the momentum mode sum, $\frac{1}{L^4}\sum_{n_\mu}$, and counts as p^4. A general Feynman diagram with I internal lines, V leading-order vertices, and L loops counts as $p^{4L-2I+2V} = p^{2L+2}$. This power counting leads to a loop expansion identical to that in infinite volume. The

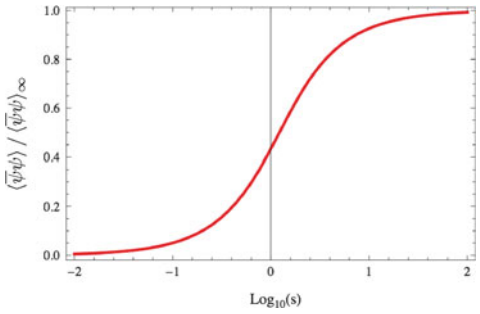

Fig. 4.6 Modification of the chiral condensate in the ε-regime. Shown as a function of the scaling variable, $s = \frac{1}{4}(fL)^2(m_\pi L)^2$, is the finite-volume depletion of the chiral condensate

essential difference is that the evaluation of Feynman graphs requires momentum-mode sums rather than momentum integrals.

Now in the p-regime, momentum-mode sums are not ideal. We prefer that contributions from loop graphs be expressed in a winding number expansion, rather than in terms of periodic momentum modes. Indeed, the external states are assumed to be projected onto good momenta; however, virtual quantum fluctuations span the range of all available momenta. Their contribution to observables is best expressed in position space. The Poisson re-summation formula allows us to recast the momentum mode sums into an expansion in winding number. Before deriving this formula, we recall the definition of the Dirac-delta function on a compact space,

$$\delta_L(x-y) = \frac{1}{L}\sum_{n=-\infty}^{\infty} e^{2\pi i n(x-y)/L}, \quad \text{for} \quad x, y \in \left(-\frac{L}{2}, \frac{L}{2}\right), \tag{4.36}$$

which by inspection has the correct $L \to \infty$ limit.

In considering loop sums, we can enforce the quantization of momentum using the Dirac comb,

$$\frac{1}{L}\sum_{n-\infty}^{\infty} \delta(k - 2\pi n/L) = \int_{-\infty}^{\infty} \frac{dx}{2\pi} e^{-ikx} \frac{1}{L}\sum_{n=-\infty}^{\infty} e^{2\pi i n x/L}, \tag{4.37}$$

where k is a continuous variable, and accordingly has a Fourier transform in terms of a noncompact variable x. We can partition the real line in terms of an infinite number of cells having length L, that is $\int_{-\infty}^{\infty} f(x)dx = \sum_{\nu=-\infty}^{\infty} \int_{\nu L - L/2}^{\nu L + L/2} f(x)dx$. Translating the latter integrals so that they are all centered about $x = 0$, we have $\int_{-\infty}^{\infty} f(x)dx = \sum_{\nu=-\infty}^{\infty} \int_{-L/2}^{+L/2} f(x - \nu L)dx$. Applying this partition to the Dirac comb, we have the Poisson formula

$$\begin{aligned}\frac{1}{L}\sum_{n-\infty}^{\infty} \delta(k - 2\pi n/L) &= \int_{-\frac{L}{2}}^{+\frac{L}{2}} \frac{dx}{2\pi} e^{-ikx} \sum_{\nu=-\infty}^{\infty} e^{ik\nu L}\, \delta_L(x) \\ &= \frac{1}{2\pi}\sum_{\nu=-\infty}^{\infty} e^{ik\nu L}.\end{aligned} \tag{4.38}$$

To utilize the Poisson formula to compute finite-volume corrections, we first observe the momentum-mode expansion of the finite-volume propagator

$$D_{\mathrm{FV}}(x,0) = \frac{1}{L}\sum_{n=-\infty}^{\infty} e^{2\pi i n x/L} G(2\pi n/L), \tag{4.39}$$

where $G(k) = [k^2 + m^2]^{-1}$ is the Euclidean momentum-space propagator in infinite volume. In light of Eq. (4.38), we have the winding-number expansion

$$D_{\mathrm{FV}}(x,0) = \sum_{\nu=-\infty}^{\infty} D_{\infty}(x+\nu L,0), \tag{4.40}$$

in terms of the infinite-volume coordinate-space propagator $D_{\infty}(x,0)$. The infinite-volume limit arises from $\nu = 0$, whereas nonzero winding numbers account for volume corrections from periodic images.

The functional form of the coordinate-space propagator is all we need to derive finite-volume corrections in the p-regime. In Euclidean space, we have the propagator

$$D_{\infty}(x,0) = \frac{m}{4\pi^2\sqrt{x^2}} K_1(m\sqrt{x^2}) \overset{x^2\to\infty}{\longrightarrow} \frac{m^2}{2(2\pi m\sqrt{x^2})^{3/2}} e^{-m\sqrt{x^2}} + \cdots \tag{4.41}$$

To compute the finite-volume modification to the chiral condensate, for example, we realize that the bubble diagram is proportional to $D_{\mathrm{FV}}(0,0)$, which can be written in the winding-number expansion using Eq. (4.40). Taking into account the $\nu = \pm 1$ images in each spatial direction gives us the result

$$\langle\overline{\psi}\psi\rangle = \langle\overline{\psi}\psi\rangle^{\infty}_{m_q=0}\left[1 + \frac{3m_\pi^2}{(4\pi f)^2}\left(\log\frac{\mu^2}{m_\pi^2} + 1 - 12\sqrt{2\pi}\frac{e^{-m_\pi L}}{(m_\pi L)^{3/2}}\right) - \frac{m_\pi^2}{f^2}L_4(\mu)\right]. \tag{4.42}$$

In this regime, corrections to the condensate are exponentially suppressed due to the propagation of pions around the world.

9 In addressing finite-volume corrections, one typically considers lattices with a finite spatial volume and infinite temporal extent. Why is this done? How would the above results be modified? Now consider the pion mass. How does it scale with volume for asymptotically large spatial volumes?

4.3.3 *Lattice Discretization Effects*

As a final application of χPT tailored to lattice QCD, we consider effects of the lattice discretization. In order to connect lattice data to QCD physics, one needs to take the continuum limit. Because χPT is a low-energy effective theory, taking the lattice spacing to zero naïvely does not play a role in the long-range physics. Most solutions to the fermion doubling problem, however, break chiral symmetry at zero

quark mass. In this way, properties of the theory's most infrared modes results from the nature of the short-distance regularization.

Near the continuum, the lattice spacing is small compared to strong-interaction scales, $a \ll \Lambda_{\rm QCD}^{-1}$, and the lattice action can be described by an effective continuum theory, know as the Symanzik effective action [18]. This theory shares all of the symmetries of the lattice action (gauge invariance, hypercubic invariance, C, P, T, ...), but is written in terms of continuum operators and organized in powers of the lattice spacing:

$$S_{\rm Symanzik} = S_0 + aS_1 + a^2 S_2 + \cdots . \tag{4.43}$$

At each order, there is a finite set of operators, $S_i = \sum_j c_j^{(i)} \mathcal{O}_j^{(i)}$, with contributions from higher-dimensional operators becoming less relevant in the continuum limit. Coefficients $c_j^{(i)}$ run weakly with logarithms of the lattice spacing. The leading-order term is just the QCD action, namely $S_0 = \overline{\psi}\left(\not{D} + m_q\right)\psi$, although fine tuning may be required to remove relevant contributions of the form $\frac{1}{a}S_{-1}$, so that the continuum limit exists. By writing Eq. (4.43), we assume any necessary fine tuning has been carried out. Notice that at leading order, Euclidean invariance accidentally appears. Operators breaking Euclidean invariance, e.g. $\overline{\psi}\gamma_\mu D_\mu D_\mu D_\mu \psi$, become irrelevant in the continuum limit.

To account for the effects of discretization on low-energy physics, we must understand how operators of the Symanzik effective action map into χPT. For illustrative early references on the subject, see [192, 193]. The Wilson action, for example, eliminates fermion doubling at the cost of explicitly breaking chiral symmetry. As a result, chiral symmetry is not imposed on the operators of Symanzik's effective action. This allows for a relevant operator, $\frac{1}{a}\overline{\psi}\psi$, that necessitates fine tuning in order to attain light quarks. After such tuning, the leading chiral symmetry breaking operator is contained in the term [194]

$$S_1 = c_{\rm SW}\left(\overline{\psi}_L \sigma_{\mu\nu} F_{\mu\nu} \psi_R + \overline{\psi}_R \sigma_{\mu\nu} F_{\mu\nu} \psi_L\right). \tag{4.44}$$

This term breaks chiral symmetry precisely the way the quark mass does, and its effects can be incorporated into χPT by including the operator

$$\Delta\mathcal{L}_{\chi\rm PT} = -a c_{\rm SW} \lambda_a \,{\rm Tr}\left(\Sigma^\dagger + \Sigma\right). \tag{4.45}$$

As a result, the pion mass depends on the lattice spacing,

$$m_\pi^2 = \tfrac{8}{f^2}\left(m_q \lambda + a\, c_{\rm SW} \lambda_a\right).$$

Infrared enhancements due to chiral logarithms now take the form

$$\sim \log[m_\pi^2(m_q, a)].$$

One should note that improvement of the action will diminish the size of the coefficient $c_{\rm SW}$, and hasten the approach to the continuum limit. Furthermore, our discussion tacitly assumes the product $c_{\rm SW}\lambda_a$ is positive, otherwise one can enter the Aoki phase [195].

Another example of discretization effects concerns mixed-action simulations. For computational economy, one can employ different lattice fermion actions for valence and sea quarks. Lattice collaborations have chosen various options so far: domain-wall valence quarks on staggered sea quarks, overlap valence quarks on domain-wall sea quarks, *etc*. The effects of a mixed action on low-energy physics can be deduced by accounting for the symmetry breaking pattern [196]. Because mixed actions distinguish between valence and sea quarks, the Symanzik effective action is a partially quenched theory. In the combined chiral and continuum limits, the partially quenched theory possesses a graded chiral symmetry, $SU(4|2)_L \otimes SU(4|2)_R$. At finite lattice spacing, however, this chiral symmetry is explicitly broken because no symmetry relates valence and sea quarks. Dimension-6 operators in the Symanzik action lead to a reduction of the chiral symmetry down to $SU(2|2)_L \otimes SU(2|2)_R \otimes SU(2)_L \times SU(2)_R$. Consequently the masses of mesons formed from one valence and one sea quark, $\phi_{\overline{\psi}\psi'}$ and $\phi_{\overline{\psi}'\psi}$ from Eq. (4.32), are not protected from additive renormalization. As a result their masses have a shift

$$\Delta(m^2_{\phi_{\overline{\psi}\psi'}}) = \Delta(m^2_{\phi_{\overline{\psi}'\psi}}) = a^2\Delta_{\rm mix} \tag{4.46}$$

that depends quadratically on the lattice spacing. The behavior of chiral logarithms is modified, but only for those generated by valence-sea meson propagation. Mixed-action χPT can be employed to understand the combined quark-mass and lattice-spacing dependence of mixed-action lattice-QCD data. For a general discussion of applications, see [197, 198].

10 Write down all dimension-6 four-quark operators in the Symanzik effective action for a general mixed-action theory. Classify the operators according to symmetry. Which ones are absent in a theory describing Wilson valence quarks and overlap sea quarks?

4.4 Including the Nucleon

To include the nucleon and other baryons in χPT, we are confronted with a puzzle. The nucleon mass is not a low-energy scale. By contrast, it is on the order of the chiral symmetry breaking scale, $M_N \approx \Lambda_\chi$. The presence of this large scale would seem to complicate the inclusion of the nucleon into χPT. One is not deriving the nucleon from chiral dynamics, however, one is investigating the effect chiral dynamics has on the nucleon. With this view in mind, we include the nucleon as an

external source of isospin and describe small energy fluctuations *about* the nucleon mass, $p \ll M_N \sim \Lambda_\chi$, as first suggested in [199].

To account for the quark-mass dependence of nucleon properties using χPT, we require the chiral-limit value of the nucleon mass, M. This quantity requires a digression. How can the chiral-limit mass M arise from nothing? In QCD, we have the energy-momentum tensor $T_{\mu\nu}$, whose matrix element between nucleon states must have the form

$$\langle N(\boldsymbol{k})|T_{\mu\nu}|N(\boldsymbol{k})\rangle = -\frac{k_\mu k_\nu}{M_N} \tag{4.47}$$

on account of Euclidean invariance and dimensional analysis. The trace of the energy-momentum tensor thus has a matrix element equal to the nucleon mass, $\langle N(\boldsymbol{k})|T_{\mu\mu}|N(\boldsymbol{k})\rangle = M_N$. At the classical level, the energy-momentum tensor's trace is simply $T_{\mu\mu} = m_q\overline{\psi}\psi$. Consequently, $M = 0$ in the chiral limit.

While these considerations apply at the classical level, QCD exhibits a trace anomaly, which is tied to the fact that QCD cannot be defined without a scale. Taking into account quantum corrections, the trace of the energy momentum tensor has the form

$$T_{\mu\mu} = \frac{\beta}{2g^3}F^A_{\mu\nu}F^A_{\mu\nu} + m_q\overline{\psi}\psi \tag{4.48}$$

with β as the QCD beta function. Due to the trace anomaly, the chiral-limit mass is nonvanishing, $M = \langle N(\boldsymbol{k})|\frac{\beta}{2g^3}F^A_{\mu\nu}F^A_{\mu\nu}|N(\boldsymbol{k})\rangle$. The Higgs mechanism does not have a monopoly over all the mass in the universe. Furthermore, on account of the trace of the energy-momentum tensor's form, we can hazard a guess about the quark-mass dependence of the nucleon mass, $M_N = M + \sigma\, m_q + \sigma_2\, m_q^2 + \cdots$, which corresponds to pion-mass dependence of the form $M_N = M + A\, m_\pi^2 + B\, m_\pi^4 + \cdots$ up to logarithms. This guess is not too far off, however, we will find further non-analytic dependence on the quark mass.

11 Is the trace of the energy-momentum tensor the divergence of a current?

4.4.1 Heavy Fermions

To work with small fluctuations about the chiral-limit value of the nucleon mass, we treat M as a large energy scale and write the nucleon momentum as $k_\mu = Mv_\mu + p_\mu$, with $p \ll M$. The uncertainty relation $\Delta k \Delta x \geq \frac{1}{2}$ becomes $\Delta v \Delta x \geq \frac{1}{2M}$ for particles of large mass, and simultaneously specifying position and velocity becomes possible.

We can see the consequences at the level of the nucleon propagator. For the free action, we have

$$\frac{1}{i\not{k}+M}=\frac{-iM\not{v}+M-i\not{p}}{2Mv\cdot p+p^2}=\frac{1}{v\cdot p}\mathcal{P}_+ +\mathcal{O}\left(\frac{p}{M}\right) \tag{4.49}$$

with the nonrelativistic projectors given by $\mathcal{P}_\pm = \frac{1}{2}(1\mp i\not{v})$. These projectors can be used to simplify the spin algebra; for example, one can easily demonstrate the identity $-\mathcal{P}_\pm\gamma_\mu\mathcal{P}_\pm = \pm iv_\mu\mathcal{P}_\pm$. Heavy-fermion propagators lead to dramatic simplifications in Feynman diagrams. Rather than rediscover these simplifications for each diagram, it is convenient to separate out the nonrelativistic modes directly at the level of the nucleon action. The relativistic fluctuations can then be integrated out of the functional integral.

To make explicit the separation of scales, we decompose the nucleon field into two parts,

$$N(x)=e^{iMv\cdot x}\left[\mathcal{P}_+ N_v(x)+\mathcal{P}_-\mathcal{N}_v(x)\right]. \tag{4.50}$$

Because of the explicit phase factor, derivatives acting on the nucleon field will produce either the large momentum, Mv_μ, or the small residual momentum p_μ. At the level of the free nucleon action, we have

$$\begin{aligned}\mathcal{L}&=\overline{N}\left(\not{\partial}+M\right)N\\&=\overline{N}_v iv\cdot\partial\mathcal{P}_+N_v-\overline{\mathcal{N}}_v\left(iv\cdot\partial-2M\right)\mathcal{P}_-\mathcal{N}_v+\text{mixing}.\end{aligned} \tag{4.51}$$

The positive projection of the nucleon, N_v, corresponds to a nonrelativistic nucleon whose energy is measured relative to zero. The negative projection, $\mathcal{N}_v$, on the other hand, corresponds to the negative-energy solution which lies $2M$ away from the positive-energy solution, see Fig. 4.7. The mixing terms between these two fields give rise to a tower of recoil corrections after the field $\mathcal{N}_v$ is integrated out.

12 Integrate out the remaining massive component of the nucleon field to find the first-order correction to the static-nucleon Lagrangian. The result should not surprise you.

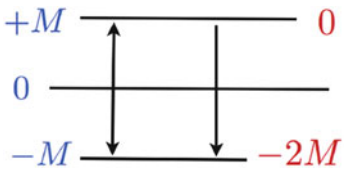

Fig. 4.7 The heavy-fermion approach repositions the zero energy level at the fermion mass M

13 The nonrelativistic projectors reduce the spin algebra to that of Pauli matrices. Show that the axial-vector fermion bilinear reduces to the spin density operator up to a constant, that is $\overline{N}_v \gamma_\mu \gamma_5 N_v = c \overline{N}_v S_\mu N_v$. The relation $\mathcal{P}_+ N_v = N_v$ will prove useful, as will the definition of the spin vector $S_\mu = -\frac{i}{4M} \varepsilon_{\mu\nu\rho\sigma} \sigma_{\nu\rho} k_\sigma$, which satisfies $S_\mu S_\mu = \frac{1}{2}\left(\frac{1}{2}+1\right)$. What are $v_\mu S_\mu$ and $[S_\mu, S_\nu]$?

4.4.2 Heavy-Nucleon χPT

With the large chiral-limit mass of the nucleon M phased away, the derivative expansion is valid: $\partial_\mu N_v \sim p$ with $p \ll M \sim \Lambda_\chi$. From this point forward, we work exclusively with the heavy-nucleon field N_v, and for notational simplicity we strip away the velocity subscript. The goal is to combine the heavy-nucleon limit with chiral perturbation theory to build a tool with which we can address the quark-mass dependence of nucleon properties, pion-nucleon interactions, and so forth.

The nucleon field is an isodoublet of the proton and neutron, $N = \begin{pmatrix} p \\ n \end{pmatrix}$. This translates into the transformation property, $N_i \to V_{ij} N_j$ under an $SU(2)_V$ transformation. On the surface, it appears that we need to know how the nucleon transforms under $SU(2)_L \otimes SU(2)_R$ in order to take into account the pattern of spontaneous and explicit chiral symmetry breaking in QCD. This situation would be unfortunate, because it is unknown to which chiral multiplets the nucleon belongs. A nice discussion and a conjecture are given in [200].

Let us temporarily assume a simple scenario for the nucleon. In the chiral limit, imagine that the nucleon has the charge assignment $(\frac{1}{2}, 0) \oplus (0, \frac{1}{2})$ under $SU(2)_L \otimes SU(2)_R$. That is, the nucleon can be written as the sum of left- and right-handed fields, N_L and N_R, which transform as $N_L \to L N_L$ and $N_R \to R N_R$ under chiral transformations. These fields can then be dressed with pions. For example, taking $\tilde{N}_L \equiv \Sigma N_R$, and $\tilde{N}_R \equiv \Sigma^\dagger N_L$, we have defined fields with exactly the same transformation properties as the original nucleon. Because pions are massless in the chiral limit, moreover, it is not possible to discern between these two possibilities. The nucleon will always be dressed with soft pion radiation, and this presents an infrared ambiguity in distinguishing between a nucleon, and a nucleon plus any number of soft pions.

To exploit the infrared ambiguity, we define the field $\xi = \sqrt{\Sigma}$. Under a chiral transformation, we have $\xi \to \sqrt{L \xi^2 R^\dagger} \equiv L \xi U^\dagger$, where U is a complicated coordinate-dependent matrix, $U = (L, R, \xi(x))$. It is simple to show that $L\xi U^\dagger = U \xi R^\dagger$. Under the vector subgroup of transformations, we have $\xi \to V \xi V^\dagger$. Now one can use the ξ field to dress the nucleon differently with pions. From our original chiral multiplet, we can define the fields $\check{N}_L = \xi N_R$ and $\check{N}_R = \xi^\dagger N_L$,

which both transform the same way, $\check{N}_L \to U\check{N}_L$ and $\check{N}_R \to U\check{N}_R$ under $SU(2)_L \otimes SU(2)_R$. Thus to whichever chiral multiplets the nucleon belongs, we can always suitably dress with pions to define a physically indistinguishable nucleon field that transforms as $N \to UN$ under chiral transformations. This transformation, moreover, respects the known vector transformation of the nucleon doublet.

We are now in a position to build the χPT Lagrangian including a heavy nucleon field. The theory described by this Lagrangian is heavy-nucleon chiral perturbation theory (HNχPT). To aid in its construction, we form the parity even and odd combinations

$$\begin{aligned}\mathcal{A}_\mu &= \frac{i}{2}\left(\xi^\dagger\partial_\mu\xi - \xi\partial_\mu\xi^\dagger\right) \to U\mathcal{A}_\mu U^\dagger \\ \mathcal{V}_\mu &= \frac{1}{2}\left(\xi^\dagger\partial_\mu\xi + \xi\partial_\mu\xi^\dagger\right) \to U\mathcal{V}_\mu U^\dagger + U\partial_\mu U^\dagger,\end{aligned} \tag{4.52}$$

where their chiral transformations are also given. From the vector-field built from mesons, $\mathcal{V}_\mu$, we can form a covariant derivative that acts on the nucleon, $D_\mu N \equiv \partial_\mu N + \mathcal{V}_\mu N$, which satisfies $D_\mu N \to U(D_\mu N)$. The $\mathcal{O}(p)$ HNχPT Lagrangian is specified by two terms

$$\mathcal{L}_{\text{HN}\chi\text{PT}} = N^\dagger iv\cdot D\, N + 2g_A N^\dagger S\cdot\mathcal{A}N. \tag{4.53}$$

The first term is the chirally covariant static-nucleon operator, which contains vector couplings of the nucleon to even numbers of pions. These couplings are exactly fixed by chiral symmetry. The second term contains spin-dependent axial-vector couplings to odd numbers of pions. These couplings are not uniquely determined in χPT, and therefore, we have assigned a low-energy constant g_A to this term (Fig. 4.8).

There are two further invariant terms at $\mathcal{O}(p)$ that we did not write down. These are $N^\dagger v_\mu N\ \text{Tr}\left(\mathcal{V}_\mu\right)$ and $N^\dagger S_\mu N\ \text{Tr}\left(\mathcal{A}_\mu\right)$. These happen to vanish, but could become relevant when flavor-singlet external fields are turned on. To include external fields, we promote the global symmetries to local ones. From left- and right-handed gauge fields, L_μ and R_μ, we form the left- and right-handed gauge-covariant derivatives, $D_{L,\mu} = \partial_\mu + iL_\mu$, and $D_{R,\mu} = \partial_\mu + iR_\mu$. These are then used to gauge the vector and axial-vector fields built from mesons:

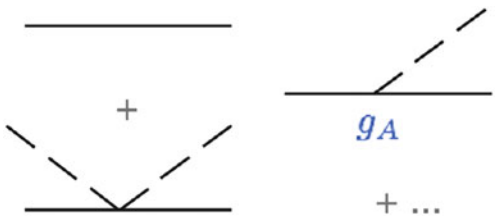

Fig. 4.8 Graphical depiction of terms from the HNχPT Lagrangian expanded to $\mathcal{O}\left(\frac{1}{f^2}\right)$. *Solid lines* denote nucleons, while the *dashed lines* denote pions

$$\mathcal{A}_\mu = \frac{i}{2}\left(\xi^\dagger D_{L,\mu}\xi - \xi D_{R,\mu}\xi^\dagger\right) \to U\mathcal{A}_\mu U^\dagger$$
$$\mathcal{V}_\mu = \frac{1}{2}\left(\xi^\dagger D_{L,\mu}\xi + \xi D_{R,\mu}\xi^\dagger\right) \to U\mathcal{V}_\mu U^\dagger + U\partial_\mu U^\dagger, \tag{4.54}$$

which have the same transformation properties as their zero-field counterparts. The leading-order HNχPT Lagrangian in external fields thus has exactly the same form up to possible flavor-singlet couplings. Turning on flavor-singlet external fields, we have simply $\mathrm{Tr}\left(\mathcal{V}_\mu\right) = \frac{i}{2}\mathrm{Tr}\left(L_\mu + R_\mu\right) = i\,\mathrm{Tr}\left(V_\mu\right)$ with V_μ the flavor-singlet vector field, and $\mathrm{Tr}\left(\mathcal{A}_\mu\right) = -\frac{1}{2}\mathrm{Tr}\left(L_\mu - R_\mu\right) = \mathrm{Tr}\left(A_\mu\right)$ with A_μ the flavor-singlet axial-vector field. The flavor-singlet vector coupling is exactly fixed by the nucleon charge assignments, $D_\mu N = \left[\partial_\mu + \mathcal{V}_\mu + \mathrm{Tr}\left(\mathcal{V}_\mu\right)\right]N$.

14 In the chiral limit, the isovector axial current is a conserved current. Is there a constraint on the quark isovector axial charge due to the non-renormalization of this current? What about on the nucleon axial charge g_A?

4.4.3 Quark-Mass Dependence of the Nucleon

To include explicit chiral symmetry breaking introduced by the quark mass, we follow the spurion trick above. It is convenient to introduce the operators

$$\mathcal{M}_\pm = \frac{1}{2}\left(\xi s^\dagger \xi \pm \xi^\dagger s\,\xi^\dagger\right) \to U\mathcal{M}_\pm U^\dagger, \tag{4.55}$$

which have the simple chiral transformations in terms of U listed. When the spurion picks up a vev, the operators become $\mathcal{M}_\pm = m_q(\Sigma \pm \Sigma^\dagger)$. The leading effects of the quark mass on the nucleon are contained in the $\mathcal{O}(p^2)$ term

$$\mathcal{L}_\mathcal{M} = \sigma\, N^\dagger \mathcal{M}_+ N. \tag{4.56}$$

Expanding this term to tree level, we find the expected linear quark-mass dependence of the nucleon mass, $M_N = M + \sigma\, m_q + \cdots$. Beyond tree-level, there are spin-independent nucleon interactions with an even number of pions contained in the above term. Pion-nucleon scattering provides an avenue to determine σ.

15 Write down all strong-isospin–breaking mass operators up to second order in the quark mass. What effect does isospin breaking in the pion mass have on the nucleon mass? Deduce the behavior of the nucleon mass splitting as a function of the quark masses.

The coefficient σ is related to an important parameter called the pion-nucleon sigma-term, which is defined by

$$\sigma_N = \frac{1}{2M_N}\langle N(\boldsymbol{k})|m_q\overline{\psi}\psi|N(\boldsymbol{k})\rangle. \tag{4.57}$$

In HNχPT, we have just established that $\sigma_N = \frac{\sigma m_q}{2M_N} + \cdots$. Determination of the sigma term is relevant for the nucleon-mass spectrum, the strangeness content of the nucleon, quark mass ratios, pion-nucleon scattering, and new-physics searches.

The sigma term is at the heart of the quark-mass dependence of the nucleon mass. Using the Feynman-Hellmann theorem, we have the relation $\sigma_N = \frac{m_q}{2M_N}\frac{\partial M_N}{\partial m_q}$, which expresses the sigma term as the incremental change in nucleon mass with respect to the quark mass. A quantity not-too-distantly related to the sigma term is the strangeness fraction in the nucleon. This fraction is defined from the ratio of matrix elements of scalar quark bilinear operators

$$y = \frac{\langle N(\boldsymbol{k})|\overline{s}s|N(\boldsymbol{k})\rangle}{\frac{1}{2}\langle N(\boldsymbol{k})|\overline{u}u + \overline{d}d|N(\boldsymbol{k})\rangle}. \tag{4.58}$$

With some algebraic rearrangement, we can produce the relation

$$\left(\frac{m_s}{m_q} - 1\right)(1-y)\,\sigma_N = \frac{m_s - m_q}{2M_N}\langle N(\boldsymbol{k})|\overline{u}u + \overline{d}d - 2\overline{s}s|N(\boldsymbol{k})\rangle \tag{4.59}$$

between quark masses, the strangeness fraction, and the pion-nucleon sigma term. The strange quark will be considered further in the next section, and we will estimate the matrix element on the right-hand side from phenomenology.

The sigma term makes an appearance in pion-nucleon scattering. In the isospin zero channel, the scattering amplitude is constrained by low-energy theorems at the Cheng-Dashen point, namely

$$\frac{1}{2}f^2 D^{I=0}(\nu = 0, t = 2m_\pi^2) - \text{Born} = \sigma_N + \text{large corrections}, \tag{4.60}$$

where the Born subtraction refers to removing contributions from nucleon intermediate states, $\pi N \to N \to \pi N$, and the large corrections scale as $\sqrt{m_q}$. The low-energy theorem can be reformulated in a faster-converging form by considering the form factor of the sigma term, $\sigma_N(t)$. In this case [201], the right-hand side can

be replaced by $\sigma_N(t = 2m_\pi^2) + \Delta_R$, where $\Delta_R \sim m_q^2$, and can be estimated using HNχPT [202]. The problem is then to compute $\sigma_N(2m_\pi^2) - \sigma_N(0)$ in order to extract the sigma term from data.

Finally, the sigma term is relevant for the detection of dark matter. In a typical direct-detection experiment, one seeks to measure the recoil of nuclei that have scattered elastically with dark matter. The scattering could be mediated through a spin-independent interaction of the form $\sim (\overline{\chi}\chi)\left(\overline{\psi}\psi\right)$, where by the dark matter particle χ is coupled to light quarks. Another potential mechanism is from dark matter coupling to the Higgs, and nuclear recoil arises from the Higgs coupling to heavy quarks, $\sim m_Q\left(\overline{Q}Q\right)H$. The Higgs coupling grows with quark mass, however, the heavy-quark scalar density in the nucleon decreases with the mass of the heavy quark. As a result, the product of the two is roughly constant for the heavy quark flavors:

$$\langle N|m_Q\overline{Q}Q|N\rangle \sim 80\ \text{MeV}\left[1 - 2\sigma_N\left(1 + \int_0^{m_s/m_q} y(x)dx\right)\right], \tag{4.61}$$

where the dominant uncertainty is not from perturbative treatment of the heavy quarks but rather from subtracting out the contribution from light quarks, see [203] for a clear discussion.

4.4.4 Beyond Leading Order

The linear quark-mass dependence of the nucleon mass is at $\mathcal{O}(p^2)$, and quadratic dependence enters at $\mathcal{O}(p^4)$ from higher-order local operators. Loop diagrams will produce non-analytic dependence on the quark mass, and the leading such contribution arises from the sunset diagram, which counts at $\mathcal{O}(p^3)$, see Fig. 4.9.

To evaluate the sunset diagram, we recall the form of the heavy-nucleon propagator in the rest frame, $v_\mu = (0, 0, 0, i)$, namely

$$D_N(x, 0) = e^{-Mx_4}\delta(\boldsymbol{x})\theta(x_4)\mathcal{P}_+, \quad \text{with} \quad \theta(x_4) = \int_{-\infty}^{\infty}\frac{dp_4}{2\pi i}\frac{e^{ip_4x_4}}{p_4 - i\epsilon}, \tag{4.62}$$

which is thus nonvanishing only for $x_4 > 0$. For the heavy-particle formulation, the pole prescription is required in Euclidean space. The heavy-nucleon propagator must be treated as $\frac{1}{p\cdot v} = \frac{-i}{p_4 - i\epsilon} = -i\mathcal{PV}\frac{1}{p_4} + \pi\delta(p_4)$ for nucleons to propagate forward in time. From this observation, we can evaluate the sunset diagram

Fig. 4.9 One-loop diagram contributing to the nucleon self energy at $\mathcal{O}(p^3)$

$$\propto \frac{g_A^2}{f^2}\int_p \frac{(p\cdot S)^2}{p\cdot v\,[p^2+m_\pi^2]} \propto \int_p \frac{(\boldsymbol{p}\cdot\boldsymbol{S})^2}{\boldsymbol{p}^2+m_\pi^2} \propto \int_p 1 - m_\pi^2 \int_p \frac{1}{\boldsymbol{p}^2+m_\pi^2}$$
$$\sim \Lambda^3 + m_\pi^2\,\Lambda + m_\pi^3, \quad (4.63)$$

where in the second line, we have introduced an ultraviolet cutoff Λ. The cubic divergence can be absorbed into the renormalized chiral-limit nucleon mass M, while the linear divergence can be absorbed into the renormalization of σ. Both of these power-law divergences are automatically subtracted in dimensional regularization. The finite piece makes a contribution to the nucleon mass that is $m_\pi^3 \propto m_q^{3/2}$. Exhibiting this contribution, we see the nucleon mass has the expansion

$$M_N = M + A\,m_\pi^2 - \frac{3\pi g_A^2}{(4\pi f)^2} m_\pi^3 + B\,m_\pi^4 \left(\log\frac{\mu^2}{m_\pi^2} + C\right) + \cdots \quad (4.64)$$

away from the chiral limit. From lattice-QCD computations of the nucleon mass, it has proven challenging to expose this behavior, see Fig. 4.10.

Chiral perturbation theory can be used to compute chiral corrections to a variety of nucleon observables, we refer the reader to an early review on the subject [205]. Of particular importance are matrix elements of quark bilinear operators, $\overline{\psi}\Gamma\psi$. These matrix elements can be parameterized in terms of various form factors, which we generically denote by $\mathcal{G}(\boldsymbol{q}^2)$, where $\boldsymbol{q}$ is a spacelike momentum transfer. The value at zero momentum transfer, $\mathcal{G}(0)$, is often a charge or a moment. The slope of the form factor away from zero momentum transfer can be used to define an *rms* radius, $\mathcal{G}(\boldsymbol{q}^2) = \mathcal{G}(0) - \frac{1}{6}\boldsymbol{q}^2\langle r_{\mathcal{G}}^2\rangle + \cdots$.

One such bilinear operator is the isovector vector current, J_μ^+. Matrix elements of this current are parameterized by

$$\langle N(\boldsymbol{p}')|J_\mu^+|N(\boldsymbol{p})\rangle = u'^\dagger\left[v_\mu G_E^+(\boldsymbol{q}^2) + \frac{i\varepsilon_{ijk}q_j\sigma_k}{2M_N}G_M^+(\boldsymbol{q}^2)\right]u, \quad (4.65)$$

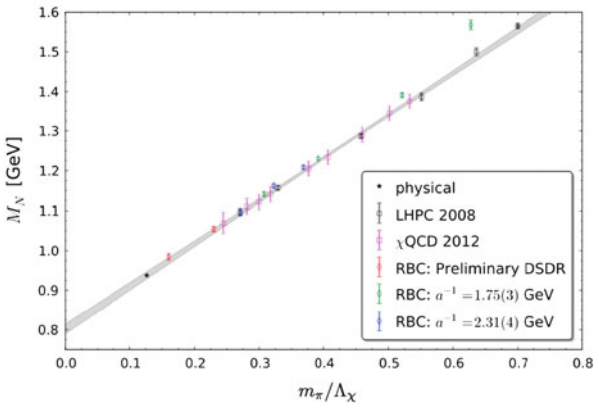

Fig. 4.10 Pion mass dependence of the nucleon mass calculated with lattice QCD. To a very good approximation, the lattice data lie along the straight line $M_N = 0.80\ \text{GeV} + m_\pi$. We thank A. Walker-Loud for providing an updated version of the plot in [204]

where G_E^+ and G_M^+ are just differences between proton and neutron electric and magnetic form factors, respectively. The isovector charge is protected from renormalization by the Ward identity. The isovector electric radius has the behavior $\langle r_E^2 \rangle = A \left(\log m_q + B \right)$ and diverges in the chiral limit. The isovector magnetic moment has the expansion $\mu_I = \mu_0 + A\, m_q^{1/2} + B\, m_q \left(\log m_q + C \right)$, while the isovector magnetic radius $\langle r_M^2 \rangle = A\, m_q^{-1/2} + B \left(\log m_q + C \right)$ also diverges in the chiral limit.

One can carry out the same analysis for the isovector axial-vector current, $J_{\mu 5}^+$. Nucleon matrix elements of this current can be parameterized in terms of two form factors, G_A and G_P,

$$\langle N(\boldsymbol{p}') | J_{\mu 5}^+ | N(\boldsymbol{p}) \rangle = 2\, u'^{\dagger} \left[S_\mu G_A(\boldsymbol{q}^2) - q_\mu \boldsymbol{S} \cdot \boldsymbol{q}\, G_P(\boldsymbol{q}^2) \right] u. \tag{4.66}$$

The axial charge of the nucleon, $G_A \equiv G_A(0)$, has a chiral expansion of the form $G_A = g_A + A\, m_q \left(\log m_q + B \right)$, while the axial radius has the expansion $\langle r_A^2 \rangle = r^2 + A\, m_q \left(\log m_q + B \right)$. The pseudoscalar form factor $G_P(\boldsymbol{q}^2)$ exhibits a pion pole

$$G_P(\boldsymbol{q}^2) = \frac{g_A}{\boldsymbol{q}^2 + m_\pi^2} - \frac{1}{6} \langle r_A^2 \rangle + \mathcal{O}\left(m_\pi^2 \right), \tag{4.67}$$

because the derivative of the isovector axial-vector current has the quantum numbers of a charged pion. Conservation of this current in the chiral limit, moreover, produces a relation between $G_A(\boldsymbol{q}^2)$ and $G_P(\boldsymbol{q}^2)$ at vanishing quark mass [206]. To contrast the behavior of axial-vector and vector form factors, we see the axial-vector size of the nucleon should be smaller than the vector size as one nears the chiral limit. The axial-vector size arises from local interactions, whereas the vector size is dominated by long-distance, charged pion loop contributions. Some credence to this picture is provided by the experimental values: $\langle r_A^2 \rangle = 0.42\ \text{fm}^2$, and $\langle r_E^2 \rangle^{p-n} = 0.88\ \text{fm}^2$.

The low-energy expansion of hadronic observables is limited by the nearest-lying states that have been excluded. For pions, such higher-lying states are reasonably well separated in energy; however, for the nucleon, the nearby $\Delta(1232)$ resonances often undermine the expansion of certain nucleon observables. The mass splitting, $\Delta \equiv M_\Delta - M_N = 290\ \text{MeV}$, is not considerably greater than the pion mass. If one imagines the strict chiral limit, $m_\pi \ll \Delta$, then these resonances can be integrated out to arrive at HNχPT. On the other hand, for physical values of the parameters, we might imagine $m_\pi \sim \Delta$, and these degrees of freedom should be retained. The size of the axial couplings $g_{\Delta N}$ and $g_{\Delta\Delta}$ gives a further phenomenological reason to include Delta-resonance degrees of freedom explicitly. Systematic inclusion of the $\Delta(1232)$ in χPT is reviewed in [207]. While one might expect the inclusion of further higher-lying resonances would improve the description of observables, these higher resonances cannot be included in a low-energy theory. Such resonances have strong decays which produce energetic pions that necessarily preclude a power-counting scheme.

4.5 Issues of Convergence

To begin this section, we remind the reader that perturbative expansions are assumed asymptotic until proven otherwise. In expanding about the chiral limit, changing the sign of the quark mass leads to vacuum instability from which we infer the chiral expansion has zero radius of convergence. This is further evidenced by the non-analyticities of χPT expressions. While the success of QED perturbation theory is set by the smallness of $\alpha = \frac{1}{137}$, the chiral expansion is far from this ideal. Often one is confronted with the need, either from lattice QCD or from phenomenology, to consider expansion parameters not considerably less than unity. For this reason, one should be aware of the limitations inherent to asymptotic series.

To illustrate these limitations, we consider a toy model provided by the integral

$$F(x) = \int_0^\infty ds \frac{e^{-s}}{1+sx}, \tag{4.68}$$

where it is assumed that $0 < x \ll 1$. For negative values of x, the integrand has a non-integrable singularity, thus any expansion about $x = 0$ has zero radius of convergence. Ignoring this fact and blindly expanding the integrand gives the series

$$F_N(x) = \sum_{n=0}^{N} (-)^n n!\, x^n, \tag{4.69}$$

which diverges as $N \to \infty$. Depending on the size of x, however, the first few terms nevertheless give a good approximation to the function $F(x)$, as shown in Fig. 4.11.

For small values of x, namely $x < \frac{1}{4}$, increasing the number of terms in the expansion from $N = 1$ to $N = 3$ gives a better approximation to the function $F(x)$. Adding further terms, however, eventually breaks the trend. Because the series has zero radius of convergence, adding further terms to the expansion limits one to a smaller range of x for which a good approximation can be obtained. For

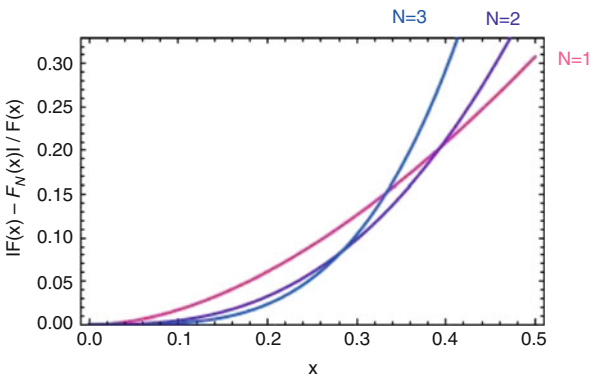

Fig. 4.11 Relative error in approximating $F(x)$ by its asymptotic expansion $F_N(x)$ for $N = 1$–3

the function at hand, the best approximation is attained for $N \sim \frac{1}{x}$. Thus to make a better approximation for larger values of x, one should actually drop higher-order terms in the expansion.

In χPT, one often goes to higher orders in the power counting to test the convergence of the expansion. Doing so, however, brings along unknown low-energy constants. If one knew the chiral-limit values of these parameters *a priori*, then one could assess the convergence. When one uses phenomenology or lattice data to fit the parameters, this task becomes considerably challenging.

In two-flavor χPT, we found that the chiral expansion of pion dynamics is governed by the small parameter $m_\pi^2/\Lambda_\chi^2 \sim 0.02$, which should still be suitably small for pion masses larger than physical. This is too idealistic in certain channels where there are resonance contributions, and more realistic expansion parameters that underlie χPT are $m_\pi^2/m_\rho^2 \sim 0.03$ and $m_\pi^2/m_\sigma^2 \sim 0.08$. When considering the chiral dynamics of the nucleon, we need the chiral limit value of the nucleon mass, which is $M = 0.80$ GeV, see Fig. 4.10. The heavy-nucleon expansion is controlled by $m_\pi/M \sim 0.2$, and Delta-resonance contributions are controlled by $m_\pi/\Delta \sim 0.5$ if excluded, and $\sqrt{\Delta^2 - m_\pi^2}/M \sim 0.3$ if included. We now investigate the state of the three-flavor chiral expansion.

4.5.1 Including Strange Mesons

The strange-quark mass is smaller than the strong-interaction scale, $m_s/\Lambda_{\rm QCD} \sim 0.3$, but not considerably so. Nevertheless, we can understand the low-energy dynamics of QCD that emerges from having three nearly massless quarks, and compare with nature.

Returning to the analysis of Sect. 4.2, the pattern of symmetry breaking in the massless three-flavor case is $SU(3)_L \otimes SU(3)_R \to SU(3)_V$, due to the formation of the chiral condensate $\langle \overline{\psi}\psi \rangle \neq 0$. The coset $SU(3)_L \otimes SU(3)_R/SU(3)_V$ is parameterized similarly to before, $\Sigma = e^{2i\phi/f}$, where $\Sigma \to L\Sigma R^\dagger$ under a three-flavor chiral transformation. The vector transformation can be used to deduce, $\phi \to V\phi V^\dagger$, and so ϕ describes an octet of mesons. These are conventionally packaged as

$$\phi = \begin{pmatrix} \frac{1}{\sqrt{2}}\pi^0 + \frac{1}{\sqrt{6}}\eta & \pi^+ & K^+ \\ \pi^- & -\frac{1}{\sqrt{2}}\pi^0 + \frac{1}{\sqrt{6}}\eta & K^0 \\ K^- & \overline{K}^0 & -\frac{2}{\sqrt{6}}\eta \end{pmatrix}. \tag{4.70}$$

The quark masses, m_q and m_s, explicitly break chiral symmetry from $SU(3)_L \otimes SU(3)_R$ down to $SU(2)_V \otimes U(1)_V$. This effect can be accounted for by the spurion trick used above. Treating each of the quark masses as $\mathcal{O}(p^2)$, the leading-order chiral Lagrangian has the form

$$\mathcal{L}_{\chi\mathrm{PT}} = \frac{f^2}{8}\,\mathrm{Tr}\left(\partial_\mu \Sigma^\dagger \partial_\mu \Sigma\right) - \lambda\,\mathrm{Tr}\left(m\,\Sigma^\dagger + m\,\Sigma\right), \tag{4.71}$$

where $m = \mathrm{diag}\,(m_q, m_q, m_s)$. Aside from this difference, the form of the Lagrangian is the same as that in the two-flavor case, although the values of the low-energy parameters f and λ are different. Their values are now determined by the three-flavor chiral limit. At $\mathcal{O}(p^4)$, there are seven Gasser-Leutwyler coefficients, and a few more when external gauge fields are included [208].

16 In the isospin limit, there are two different quark masses but three different meson masses in the pseudoscalar octet. Use the three-flavor chiral Lagrangian to derive the constraint,

$$\Delta_{\mathrm{GMO}} = \frac{4}{3}m_K^2 - m_\eta^2 - \frac{1}{3}m_\pi^2 = 0, \tag{4.72}$$

which was originally found by Gell-Mann and Okubo. What happens away from the isospin limit?

The tree-level masses of the pseudoscalar mesons lead to the relation $\Delta_{\mathrm{GMO}} = 0$ in Eq. (4.72). Inserting the neutral-meson masses and dividing by the average octet-meson mass, we see that experimentally $\Delta_{\mathrm{GMO}}/\overline{m}_\phi^{\,2} \sim 0.15$. Beyond tree level, this relation is modified by one-loop mass corrections, and local counterterms from the $\mathcal{O}(p^4)$ Lagrangian. Estimating the size of such corrections leads to $\Delta_{\mathrm{GMO}} \sim \frac{m_\phi^4}{\overline{m}_\phi^2 \Lambda_\chi^2}$. In $SU(3)$ χPT, the η meson is the most worrisome. Fourth-order contributions from the η should be $\sim 35\,\%$. This is about the size of corrections needed for the Gell-Mann–Okubo relation, but notice that a factor of two can seriously upset the situation.

To expand about the three-flavor chiral limit, we must add to $m_\pi^2/\Lambda_\chi^2 \sim 0.02$ two further expansion parameters, $m_K^2/\Lambda_\chi^2 \sim 0.23$ and $m_\eta^2/\Lambda_\chi^2 \sim 0.27$. Pending unfortunate numerical factors, $\mathcal{O}(p^6)$ contributions to meson quantities (which include two-loop diagrams) should be $\sim 10\,\%$. To work at this order, one must introduce ~ 100 low-energy constants, which makes it difficult to address issues of convergence. The comprehensive study of χPT predictions at next-to-next-to-leading order allows one to form relations sensitive to only $\mathcal{O}(p^6)$ low-energy constants. While most are not well known, one can use these relations to assess the convergence of the three-flavor expansion, with the result that the expansion "mostly works" [209].

17 Revisit electromagnetic mass corrections in three-flavor χPT. Find all leading- and next-to-leading-order electromagnetic mass operators. Ignoring the up- and down-quark masses, which octet-meson masses are affected by leading and next-to-leading operators?

18 Accounting for strong and electromagnetic isospin breaking to leading order, compute the mass spectrum of the meson octet using χPT. Devise a way to determine the quark mass ratios m_u/m_d and m_d/m_s using the experimentally measured meson masses.

4.5.2 Including Strange Baryons

The lowest-lying baryons form an octet under $SU(3)_V$ and can be packaged in the matrix

$$B = \begin{pmatrix} \frac{1}{\sqrt{2}}\Sigma^0 + \frac{1}{\sqrt{6}}\Lambda & \Sigma^+ & p \\ \Sigma^- & -\frac{1}{\sqrt{2}}\Sigma^0 + \frac{1}{\sqrt{6}}\Lambda & n \\ \Xi^- & \Xi^0 & -\frac{2}{\sqrt{6}}\Lambda \end{pmatrix}, \tag{4.73}$$

which accordingly transforms as $B \to VBV^\dagger$. While the chiral multiplets for these baryons in the chiral limit are unknown, we are free to choose the $SU(3)_L \otimes SU(3)_R$ transformation $B \to UBU^\dagger$ due to the ambiguity in resolving a baryon, and a baryon plus any number of soft octet mesons.

In the three-flavor chiral limit, the octet baryons are degenerate, with a mass we denote by M_B. This mass must be treated as a large scale, and the baryon fields decomposed into heavy baryon fields. Their interactions with octet mesons are constrained by the form of spontaneous and explicit breaking of chiral symmetry. Construction of the heavy-baryon chiral perturbation theory (HBχPT) Lagrangian proceeds similarly to that for the heavy nucleon. To aid in the construction, we appeal to the vector and axial-vector fields built from mesons, $\mathcal{V}_\mu$ and $\mathcal{A}_\mu$ in Eq. (4.52). The former can be used to build a chirally covariant derivative, $D_\mu B \equiv \partial_\mu B + \big[\mathcal{V}_\mu, B\big]$, which transforms as $D_\mu B \to U\left(D_\mu B\right)U^\dagger$.

To $\mathcal{O}(p)$, we have the gauged static-baryon term and two independent axial interactions,

$$\mathcal{L}_{\text{HB}\chi\text{PT}} = \text{Tr}\left(B^\dagger iv\cdot D\, B\right) + 2D\,\text{Tr}\left(B^\dagger S_\mu\{\mathcal{A}_\mu, B\}\right) + 2F\,\text{Tr}\left(B^\dagger S_\mu[\mathcal{A}_\mu, B]\right). \tag{4.74}$$

Further terms are required at $\mathcal{O}(p)$ because of the nearness of spin-$\frac{3}{2}$ baryon resonances. These baryons form a decuplet under $SU(3)_V$, so that $T_{ijk} \to V_i^{i'} V_j^{j'} V_k^{k'} T_{i'j'k'}$, with T_{ijk} completely symmetric. The size of the average mass splitting between the octet and decuplet baryons, $\Delta \equiv M_T - M_B = 270\,\text{MeV}$, necessitates inclusion of the decuplet because $\Delta \sim \overline{m}_\phi$. Their leading-order Lagrangian is given by

$$\mathcal{L}^{(\Delta)}_{\text{HB}\chi\text{PT}} = T^\dagger_\mu \left(iv\cdot D + \Delta\right) T_\mu + 2H\, T^\dagger_\mu S\cdot \mathcal{A} T_\mu + 2C\, \left(T^\dagger_\mu \mathcal{A}_\mu B + B^\dagger \mathcal{A}_\mu T_\mu\right) \tag{4.75}$$

and includes an axial coupling of pions to the decuplet H, as well as an axial transition coupling of pions to octet and decuplet baryons C. Notice the large mass scale M_B has been removed from the chiral-limit decuplet mass rather than M_T. While we could remove the mass of the decuplet fields, the splitting Δ would then show up in time-dependent factors for the axial baryon transition, and these factors would ultimately incorporate the baryon mass difference in Feynman diagrams which involve both octet and decuplet baryons.

To include the leading-order effects of quark masses, we need terms of the $\mathcal{O}(p^2)$ Lagrangian. Focusing on the quark-mass dependence of the octet baryons, we have three leading-order terms

$$\mathcal{L}_m = b_D\,\text{Tr}\left(B^\dagger\{\mathcal{M}_+, B\}\right) + b_F\,\text{Tr}\left(B^\dagger[\mathcal{M}_+, B]\right) + b_\sigma\,\text{Tr}\left(B^\dagger B\right)\,\text{Tr}\left(\mathcal{M}_+\right). \tag{4.76}$$

Because there are three parameters and four octet baryon masses in the isospin symmetric limit, there is a relation between the masses implied by leading-order HBχPT, which has the form

$$M_{\text{GMO}} = M_\Lambda + \frac{1}{3}M_\Sigma - \frac{2}{3}M_N - \frac{2}{3}M_\Xi = 0. \tag{4.77}$$

Experimentally, this relation is very well satisfied. Normalizing to the average octet-baryon mass, we have $M_{\text{GMO}}/\overline{M}_B \sim 1\,\%$. Corrections to this relation can be computed in HBχPT and first arise at $\mathcal{O}(p^3)$ from one-loop diagrams. Because these contributions are non-analytic in the quark masses, there are no additional parameters required beyond the various axial couplings entering the one-loop diagrams.

To compute the one-loop corrections, we require the octet-baryon sunset diagram, shown in Fig. 4.9. This diagram evaluates similarly to before. Additionally, we require the sunset diagram shown in Fig. 4.12. The anatomy of this intermediate-state decuplet contribution is as follows. By angular momentum, the virtual meson must be in a relative p-wave, which at low energies requires the momentum suppression factor $\boldsymbol{p}^{2\ell}$ with $\ell = 1$. This factor automatically appears in the numerator when evaluating the Feynman diagram:

Fig. 4.12 One-loop octet-baryon (B) self-energy diagram with intermediate-state decuplet (T) baryon

$$\sim \frac{C^2}{f^2}\int_p \frac{\boldsymbol{p}^2}{[ip_4+\Delta][(p_4)^2+\boldsymbol{p}^2+m_\phi^2]}. \tag{4.78}$$

The energy integral can be done by contour integration, which puts the meson on shell with $E_\phi = \sqrt{\boldsymbol{p}^2+m_\phi^2}$. The diagram is then proportional to

$$\frac{C^2}{f^2}\int_{\boldsymbol{p}} \frac{\boldsymbol{p}^2}{E_\phi(E_\phi+\Delta)} \sim \frac{C^2}{f^2}\int_{m_\phi}^{\Lambda} dE_\phi \frac{(E_\phi^2-m_\phi^2)^{3/2}}{E_\phi+\Delta}, \tag{4.79}$$

where the numerator factor is a combination of p-wave suppression, $\boldsymbol{p}^2 = E_\phi^2 - m_\phi^2$, and the available two-body phase space near threshold, $\sqrt{E_\phi^2-m_\phi^2}$. In changing variables, we have included an ultraviolet cutoff Λ to regulate the divergences. For large meson energies, there are multiple divergences,

$$\begin{aligned}&\int^{\Lambda} dE\, E^2 \left(1-\frac{\Delta}{E}+\frac{\Delta^2}{E^2}-\frac{\Delta^3}{E^3}+\cdots\right)\left(1-\frac{3}{2}\frac{m_\phi^2}{E^2}+\cdots\right)\\ &\sim \Lambda^3+\Delta\Lambda^2+\Delta^2\Lambda+\Delta^3\log\Lambda+m_\phi^2\,\Lambda+m_\phi^2\,\Delta\log\Lambda+\text{finite}.\end{aligned} \tag{4.80}$$

The first four terms are removed by the chiral-limit baryon-mass renormalization condition, $M_{N,\Sigma,\Lambda,\Xi}\Big|_{m_q=m_s=0} = M_B$. The remaining two divergences are proportional to the quark masses. The first is a power-law divergence which can be removed by a renormalization of the parameters $b_{D,F,\sigma}$. The logarithmic divergence produces running of these couplings, which is possible due to treating Δ as a small parameter. After renormalization, what remains is described by $\mathcal{F}(m_\phi,\Delta,\mu)$, which is a non-analytic function of m_ϕ and Δ that is given by

$$\begin{aligned}\mathcal{F}(m,\delta,\mu) = (m^2-\delta^2)\left[\sqrt{\delta^2-m^2}\log\left(\frac{\delta-\sqrt{\delta^2-m^2+i\epsilon}}{\delta+\sqrt{\delta^2-m^2+i\epsilon}}+\delta\log\frac{\mu^2}{m^2}\right)\right]\\ +\frac{1}{2}\delta m^2\log\frac{\mu^2}{m^2}+\delta^3\log\frac{\mu^2}{4\delta^2}.\end{aligned} \tag{4.81}$$

For $\delta > -m$, the function $\mathcal{F}(m,\delta,\mu)$ is real valued.

Table 4.1 Estimated one-loop correction to the baryon Gell-Mann–Okubo relation

Source	D	F	C	$M_{\rm GMO}/\overline{M}_B$
χPT [210]	0.61	0.40	1.2	0.79 %
Lattice QCD [211]	0.72	0.45	1.6	1.12 %
SU(6) Quark Model	3/4	1/2	3/2	1.29 %

Combining results for the two sunsets, and forming the linear combination of octet baryon masses in Eq. (4.77), we have the one-loop result

$$M_{\rm GMO} = \frac{4}{3(4\pi f)^2}\left[\pi(D^2-3F^2)\Delta_{\rm GMO}(m_\phi^3) - \frac{1}{6}C^2\Delta_{\rm GMO}[\mathcal{F}(m_\phi,\Delta,\mu)]\right], \tag{4.82}$$

where $\Delta_{\rm GMO}(x_\phi) = \frac{4}{3}x_K - x_\eta - \frac{1}{3}x_\pi$ for any octet-baryon quantity x, and consequently the μ dependence is only superficial. The one-loop correction is determined using various estimates of the axial couplings, see Table 4.1, and is in line with the experimental value for $M_{\rm GMO}$. This agreement is actually quite surprising if we analyze the expansion of individual octet baryon masses. The one-loop corrections are particularly large: for the nucleon, $\delta M_N(\mu = \Lambda_\chi)/M_N = -39\,\%$; for the Lambda hyperon, $\delta M_\Lambda(\mu = \Lambda_\chi)/M_\Lambda = -67\,\%$; for the Sigmas, $\delta M_\Sigma(\mu = \Lambda_\chi)/M_\Sigma = -89\,\%$; and finally for the cascade baryons, $\delta M_\Xi(\mu = \Lambda_\chi)/M_\Xi = -98\,\%$. The expansion is worse with increasing strangeness because of larger couplings to strange mesons. The expansion parameters governing the heavy-octet-baryon expansion are not considerably less than unity, m_K/M_B and m_η/M_B are both ~ 0.5. The success of three-flavor HBχPT to describe certain observables seems to require a deeper explanation.

19 Recall the relation between the nucleon sigma term and strangeness, Eq. (4.59). Using the baryon chiral Lagrangian at tree level, calculate the matrix element on the right-hand side and express it in terms of the octet baryon masses. Finally, obtain a rough estimate the size of the sigma term.

4.5.3 Excluding Strangeness

In the three-flavor chiral expansion, we treat the quark masses equally $m_q \sim m_s \ll \Lambda_{\rm QCD}$. Unless one is exceptionally lucky, the strange-quark mass is probably too large to be considered a perturbation about the chiral limit. With notable exceptions, baryon observables exhibit poor convergence, and even meson properties determined with lattice QCD extrapolate better without the constraints of $SU(3)$ χPT [212].

One approach to the problematic strange quark is to integrate it out in order to use a two-flavor chiral expansion. This corresponds to the mass hierarchy $m_q \ll m_s \sim \Lambda_{\rm QCD}$. For the nucleon and pion, integrating out the strange quark results in $SU(2)$ χPT developed above. For the nucleon, we treated it as an external source of isospin, and nothing stops us from having external sources with nonvanishing strangeness quantum number. As a result, one can consider $SU(2)$ χPT for strange hadrons [213–215]. This description has limited predictive power, but is ideally suited for lattice applications.

To exhibit the idea behind two-flavor chiral expansions for strange hadrons, consider the kaon mass. At tree level in $SU(3)$, one has the expression

$$m_K^2 = \frac{4\lambda}{f^2}\left(m_q + m_s\right) = \frac{1}{2}m_\pi^2 + M_K^2 = M_K^2\left(1 + \frac{m_\pi^2}{2M_K^2} + \cdots\right), \tag{4.83}$$

where we have separated out dependence on the strange quark mass by defining the two-flavor chiral-limit value of the kaon mass, $M_K = m_K\big|_{m_q=0}$. From the physical kaon mass, $m_{K^0} = 0.497$ GeV, we can estimate M_K using $SU(3)$ χPT at one-loop order. Not surprisingly, the overwhelming majority of the kaon mass arises from the strange quark, $M_K = 0.486(5)$ GeV, where the uncertainty corresponds to that from the fourth-order low-energy constants.

Now we extend the idea to hyperons. Consider for simplicity kaon contributions to the mass of the Σ baryon. These contributions schematically take the form

$$\begin{aligned} M_\Sigma &= M_B + a\, m_K^2 + b\, m_K^3 + \cdots \\ &= M_B + a' M_K^2 + a'' m_\pi^2 + b' M_K^3 + b'' M_K m_\pi^2 + b''' \frac{1}{M_K} m_\pi^4 + \cdots, \end{aligned} \tag{4.84}$$

where, in the second line, we have expanded out the contributions from the strange-quark mass. This expression can then be reorganized into an $SU(2)$ chiral-limit expansion,

$$M_\Sigma = M_\Sigma^{(2)} + A\, m_\pi^2 + B\, m_\pi^3 + C\, m_\pi^4 \left(\log m_\pi + D\right) + \cdots, \tag{4.85}$$

where $M_\Sigma^{(2)}$ denotes the Σ baryon mass in the two-flavor chiral limit. In the $SU(2)$ expansion, the all-orders strange-quark mass dependence is contained in the parameters, $M_\Sigma^{(2)}, A, B, \ldots$

The price to pay for a better converging expansion is a mild proliferation of low-energy constants. Table 4.2 summarizes the various parameters entering the two-flavor expansion of baryon properties. Computing the one-loop contributions to baryon masses in two-flavor χPT and evaluating these at a scale of $\mu = \Lambda_\chi$ shows perturbatively small corrections over a range of pion masses, see Fig. 4.13. The dimensionless parameters underlying the two-flavor chiral expansion are m_π^2/Λ_χ^2 and m_π^2/M_K^2, and $m_\pi/M^{(2)}$ from the heavy-baryon expansion. Baryons

Table 4.2 Comparison of $SU(3)$ and $SU(2)$ χPT for baryons. Listed for each theory are the quantities required to be small for the perturbative expansion, the baryon multiplets entering the theory, and their associated axial couplings

	$SU(3)$	$SU(2)_{S=0}$	$SU(2)_{S=1}$	$SU(2)_{S=2}$	$SU(2)_{S=3}$
Expansion	p	p	p	p	p
Parameters	m_π, m_K, m_η	m_π	m_π	m_π	m_π
	Δ	$\Delta_{\Delta N}$	$\Delta_{\Sigma\Lambda}, \Delta_{\Sigma^*\Sigma}$	$\Delta_{\Xi^*\Xi}$	
Baryon	**8** B	**2** N	**1** Λ, **3** Σ	**2** Ξ	
Multiplets	**10** T	**4** Δ	**3** Σ^*	**2** Ξ^*	**1** Ω
Axial	D, F	g_A	$g_{\Lambda\Sigma}, g_{\Sigma\Sigma}$	$g_{\Xi\Xi}$	
Couplings	C	$g_{\Delta N}$	$g_{\Lambda\Sigma^*}, g_{\Sigma\Sigma^*}$	$g_{\Xi\Xi^*}$	
	H	$g_{\Delta\Delta}$	$g_{\Sigma^*\Sigma^*}$	$g_{\Xi^*\Xi^*}$	

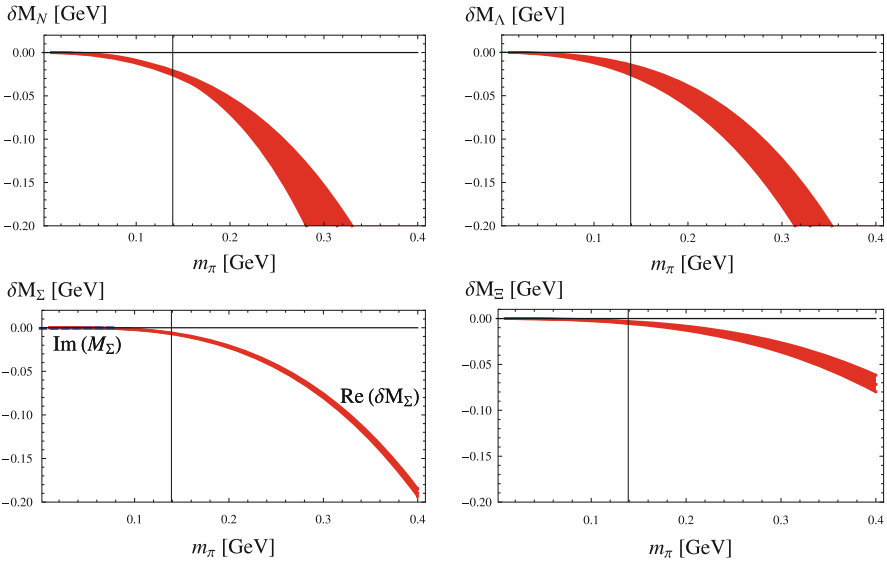

Fig. 4.13 One-loop corrections to baryon masses as functions of pion mass in $SU(2)$ HBχPT. The bands are generated by varying the renormalization scale μ within $\pm 25\,\%$ of Λ_χ

with increasing strangeness perform correspondingly better in $SU(2)$ χPT for two reasons. The first reason is that the axial couplings decrease with increasing strangeness. Secondly the heavy baryon approximation depends on the $SU(2)$ chiral-limit masses, and these increase with increasing strangeness. As a result, the approximation works better the stranger the hyperon. Lattice QCD will ultimately reveal whether this is a successful description of hyperons, and whether $SU(3)$ relations among couplings emerge.

20 Use $SU(2)$ χPT to construct a low-energy theory of kaons. Do the same for the η.

21 Find a process involving strange baryons for which a description in terms of $SU(2)$ χPT must certainly fail.

4.5.4 Not-So-Heavy Baryons

Treating baryons as heavy is required to have a power counting scheme, however, the static approximation is often severe. Recoil corrections can be treated in perturbation theory, but this approach will not allow one to exactly capture the correct analytic structure of amplitudes. Most unnerving, furthermore, is that the heavy-baryon approximation can lead to unphysical singularities. In such cases, one needs all-orders re-summation of recoil corrections, and this can be achieved through relativistic-baryon χPT [216].

We will use the nucleon's scalar form factor as an illustrative example. Using relativistic nucleon spinors, this form factor is defined from the matrix element

$$\langle N(\boldsymbol{p}')|m_q\left(\overline{u}u+\overline{d}\,d\right)|N(\boldsymbol{p})\rangle=\overline{u}(\boldsymbol{p}')\sigma(t)u(\boldsymbol{p}) \tag{4.86}$$

and differs by a trivial normalization factor from the scalar form factor we used in Sect. 4.4, namely $\sigma_N(t)=\frac{1}{2M_N}\sigma(t)$. Computing this matrix element at the Cheng-Dashen point ($t=2m_\pi^2$) with HNχPT, we obtain the result $\sigma(t=2m_\pi^2)-\sigma(t=0)=\frac{3\pi g_A^2 m_\pi^3}{2\Lambda_\chi^2}$ with corrections at $\mathcal{O}(m_\pi^4)$. This result does not indicate anything problematic about the heavy-nucleon approach.

For a general t-channel momentum transfer, the analytic properties of the amplitude allow for a once-subtracted dispersion relation,

$$\sigma(t)-\sigma(0)=\frac{t}{\pi}\int_{4m_\pi^2}^{\infty}dt'\,\frac{\mathcal{I}[\sigma(t')]}{t'(t'-t)}, \tag{4.87}$$

where the integration proceeds along the two-pion cut. The fully relativistic computation at one loop can be obtained using the imaginary part of the form-factor diagrams with relativistic kinematics and the dispersion integral above. The result has the form

$$\sigma(t)-\sigma(0)=\frac{3\pi g_A^2 m_\pi}{4\Lambda_\chi^2} \tag{4.88}$$
$$\left[(t-2m_\pi^2)\left[\frac{1}{2\sqrt{\tau}}\log\frac{1+\sqrt{\tau}}{1-\sqrt{\tau}}-\log\left(1+\frac{m_\pi}{2M_N\sqrt{1-\tau}}\right)\right]\right.$$
$$\left.+2m_\pi^2\left[1-\log\left(1+\frac{m_\pi}{2M_N}\right)\right]\right].$$

Above, τ is the threshold parameter defined by $\tau=\frac{t}{4m_\pi^2}$.

One can perform the same computation using HNχPT. This result agrees with the heavy-nucleon limit, $m_\pi/M_N \ll 1$, of the fully relativistic expression, which is given by

$$\sigma(t)-\sigma(0)=\frac{3\pi g_A^2 m_\pi}{4\Lambda_\chi^2}\left[(t-2m_\pi^2)\left[\frac{1}{2\sqrt{\tau}}\log\frac{1+\sqrt{\tau}}{1-\sqrt{\tau}}\right]+2m_\pi^2\right], \tag{4.89}$$

where the second term survives at the Cheng-Dashen point. The problem with the above expression, however, is that it becomes singular at the two-pion threshold. This unphysical behavior is due to the factor $\frac{1}{2}\log\frac{1+\sqrt{\tau}}{1-\sqrt{\tau}} \to -\frac{1}{2}\log(1-\tau)$, as $\tau \to 1$. Physically, we expect a branch cut to start at threshold, whereas HNχPT produces an unphysical singularity right at threshold.

The fully relativistic expression has the correct analytic structure. As one approaches threshold, the unphysical singularity is exactly canceled by the additional logarithm in Eq. (4.88), namely $-\log\left(1+\frac{m}{2M_N\sqrt{1-\tau}}\right) \to +\frac{1}{2}\log(1-\tau)$. This logarithm, moreover, is responsible for the branch cut above threshold. The complications with the heavy-nucleon approach can be linked to the emergence of a large parameter as one nears threshold. This parameter is $\frac{m_\pi}{M_N\sqrt{1-\tau}}$, which is small in the heavy-nucleon approach, $m_\pi/M_N \ll 1$, but the strict heavy-nucleon power counting is spoiled as one nears threshold, $\tau \to 1$. Consequently re-summation of m_π/M_N terms becomes necessary to produce the physically correct analytic behavior of the form factor.

If one requires χPT amplitudes in the vicinity of multiparticle thresholds, one must be careful to perform re-summations to produce the correct non-analyticities. On the other hand, when one is far from such thresholds, their effect can be captured in a tower of analytic terms. This is the principle underlying the construction of every effective field theory.

4.6 Final Remarks

To conclude, we will summarize the results detailed in this chapter in just a few sentences. χPT provides the tool to systematically account for the light-quark–mass dependence of low-energy QCD observables. This effective field theory is written in terms of the approximate Nambu-Goldstone modes that emerge from spontaneous breaking of chiral symmetry. Their interactions, and interactions with low-lying baryons are constrained by the symmetries and symmetry-breaking pattern of QCD. The perturbative expansion of χPT is limited in practice by the size of the physical quark masses relative to strong interaction scales. The nonrelativistic-baryon approximation, and, in particular, the size of the strange-quark mass put strain on the expansion.

Prior to lattice-QCD computations, χPT was the only way to do precision low-energy QCD phenomenology. The era of high-precision lattice QCD has altered the situation. Lattice gauge theory and chiral dynamics have been used in conjunction as an essential way to extract physics from QCD. In the next era, we see lattice computations testing the rigor of the chiral expansion directly, with the power of resolving long-standing puzzles. As our understanding progresses beyond the single-nucleon sector, we additionally may hope to expose the chiral dynamics of light nuclei from first principles.

Acknowledgements Work supported by a joint City College of New York – RIKEN/Brookhaven Research Center fellowship, an award of the Professional Staff Congress of the City University of New York, the Alfred P. Sloan foundation through a City University of New York Junior Faculty Research Award in Science and Engineering, and by the U.S. National Science Foundation, under grant number PHY12-05778.